

This author's accepted manuscript may be used for non-commercial purposes in accordance with [Wiley Terms and Conditions for Self-Archiving](#).

The full details of the published version of the article are as follows:

TITLE: Second tectofugal pathway in a songbird (*Taeniopygia guttata*) revisited: Tectal and lateral pontine projections to the posterior thalamus, thence to the intermediate nidopallium

AUTHORS: J. Martin Wild, Andrea H. Gaede,

JOURNAL: Journal of Comparative Neurology

PUBLISHER: Wiley

PUBLICATION DATE: 19 August 2015

DOI: <https://doi.org/10.1002/cne.23886>

The second tectofugal pathway in a songbird (*Taeniopygia guttata*) revisited: tectal and lateral pontine projections to the posterior thalamus, thence to the intermediate nidopallium

J. Martin Wild, Department of Anatomy with Radiology, Faculty of Medical and Health Sciences, University of Auckland, Auckland, New Zealand, and
Andrea H. Gaede, Department of Zoology, University of British Columbia, Vancouver, Canada.

46 text pages and 9 figures

Key words: zebra finch, tecto-thalamic, ponto-thalamic, tecto-pontine, and ponto-cerebellar projections

Running head: Second tectofugal pathway in a songbird

Grant sponsor: Human Frontiers Science Program, Grant RPF0012/2010;

Grant Sponsor: National Institutes of Health, Grant number 2 R01 NS029467-16A2 to R.A. Suthers, Indiana University.

Author contributions: JMW planned the study, carried out all the experiments, analysed the results, and wrote the paper. AHG contributed to some of the experiments, assisted with the analysis and interpretation of results, and drew the figures in Adobe Illustrator.

Conflict of interest: The authors declare no conflict of interest

Email: jm.wild@auckland.ac.nz

Abstract

Birds are almost always said to have two visual pathways from the retina to the telencephalon: thalamofugal terminating in the Wulst, and tectofugal terminating in the entopallium. Often ignored is a second tectofugal pathway that terminates in the nidopallium medial to and separate from the entopallium (e.g., Gamlin and Cohen, *J Comp Neurol*, 250: 296-310, 1986). Using standard tract tracing and electroanatomical techniques, we extend earlier evidence of a second tectofugal pathway in songbirds (Wild, *J Comp Neurol*, 349:512-535, 1994), by showing that visual projections to nucleus uvaeformis (Uva) of the posterior thalamus in zebra finches extend farther rostrally than to Uva as generally recognized in the context of the song control system. Projections to 'rUva' resulted from injections of biotinylated dextran amine into the lateral pontine nucleus (PL), and led to extensive retrograde labeling of tectal neurons, predominantly in layer 13. Injections in rUva also resulted in extensive retrograde labeling of predominantly layer 13 tectal neurons, retrograde labeling of PL neurons, and anterograde labeling of PL. It thus appears that some tectal neurons could project to rUva and PL via branched axons.

Ascending projections of rUva terminated throughout a visually responsive region of the intermediate nidopallium (NI) lying between nucleus interface medially and the entopallium laterally. Lastly, as shown by Clarke in pigeons (*J Comp Neurol*, 174:535-552, 1977), we found that PL projects to caudal cerebellar folia.

Although tectofugal and thalamofugal visual pathways have been well described and reviewed in the avian literature (e.g., Karten and Revzin, 1966; Karten and Hodos, 1970; Karten et al., 1973; Engelage and Bischof, 1993; Shimizu and Bowers, 1999; Shimizu and Karten, 2003; Shimizu et al., 2008; 2010), a much less well recognized, second tectofugal visual pathway was clearly demonstrated in pigeons by Gamlin and Cohen (1986) and in finches by Wild (1994). This pathway originates in several deep laminae of the optic tectum, but primarily in lamina 13. These cells project, predominantly ipsilaterally, upon the posterior thalamus, specifically upon the caudal part of nucleus dorsolateralis posterior (DLPc) in pigeons or nucleus uvaeformis (Uva) in songbirds, these two nuclei therefore being considered homologous as tectorecipient and other sensory-recipient nuclei in aves (Wild, 1994). Other lamina 13 cells originate the better known first tectofugal projection to the thalamic nucleus rotundus (Rt) and thence to the entopallium (E: Karten and Revzin, 1966; Karten and Hodos, 1970; Benowitz and Karten, 1976; Karten et al., 1997; Marin et al., 2003; Fredes et al., 2010).

In pigeons DLPc projects to the caudal part of the intermediate nidopallium (NI) where the major terminal field lies immediately dorsal to the raised medial angle of the lamina pallio-subpallialis (PSP = old lamina medullaris dorsalis, LMD: Kitt and Brauth, 1982; Gamlin and Cohen, 1986; Wild, 1987a; Funke, 1989). A minor DLPc terminal field occupies the dorsal nidopallium (Wild, 1994) and diffuse terminations have been localized to the lateral part of the caudal nidopallium (NCL: Güntürkün and Kröner, 1999). Neurons in the major DLPc terminal field in NI then project upon the same region of the dorsal nidopallium as do those in DLPc (Wild, 1994).

A similar series of projections is found in songbirds, in which they form part of the song system. The equivalent of the major DLPc terminal is called nucleus interface (Nif), which receives its thalamic projection from Uva (Nottebohm et al., 1982; Wild, 1994). Both Uva and Nif then project directly to HVC in the dorsal nidopallium (Nottebohm et al., 1982; Wild, 1994).

Functionally, DLPc in pigeons and Uva in songbirds receive multimodal ascending sensory inputs from similar sources: visual from the tectum (Hunt and Künzle, 1976; Gamlin and Cohen, 1986; Korzeniewska and Güntürkün, 1990; Wild, 1994), somatosensory from the dorsal column and external cuneate nuclei (Wild, 1989; 1994; Korzeniewska and Güntürkün, 1990), and auditory inputs from an unknown source in pigeons (Korzeniewska, 1987; Korzeniewska and Güntürkün, 1990) but from the ventral nucleus of the lateral lemniscus in zebra finches (Coleman et al., 2007) (Fig. 9). Within DLPc's major terminal field in NI, and in Uva's terminal field in Nif, robust somatosensory and visual responses have been recorded (Wild, 1987a; 1994; Funke, 1989). In the context of song control, however, Nif is now considered the principal source of auditory input to the vocal control nucleus HVC, via inputs from the caudal mesopallium (CM: Vates et al., 1996; Lewandowski et al., 2013). In pigeons more rostral regions of DLP (DLPr) project farther rostrally and laterally in NI, where they terminate medially adjacent to the entopallium (Gamlin and Cohen, 1986), or more dorsally in the medial part of NI (NIM: Güntürkün and Kröner, 1999). Physiological recordings from these regions are not available, but it can be noted that the nucleus DLPr, which previously had been thought to be somatosensory, is the target of vestibular and lateral cerebellar projections (Wild, 1988; Arends and Zeigler, 1991). In zebra finches, more rostral parts of Uva also

project to more rostral and lateral parts of NI, where visual responses have been recorded (Wild, 1994).

In the present study we extend previous observations of the afferent and efferent projections of Uva (Wild, 1994; Akutagawa and Konishi, 2005; 2010). We show that tectal inputs to Uva also extend rostral to Uva (i.e., to rUva) and that the lateral pontine nucleus (PL) also provides an input to the Uva/rUva complex, both directly, and possibly via collaterals of tectal neurons that also innervate PL. In addition, we demonstrate outputs from rUva to a large visually responsive region lying between the entopallium laterally and NIf medially. Finally, we show that PL in the zebra finch, like PL in pigeons (Clarke, 1977) projects upon caudal cerebellar folia.

MATERIALS AND METHODS

Subjects

Fifty adult (>100 days) male and female zebra finches, obtained from commercial sources, were used. Each was anesthetized by an injection of an equal parts mixture of ketamine hydrochloride (50 mg/kg) and xylazine (20 mg/kg) in the pectoral muscles and the head fixed in a David Kopf stereotaxic apparatus with ear and beak bars. However, the ear bars were not inserted deep into the external auditory meatus (e.g., as required for pigeons: Karten and Hodos, 1967), but were fashioned such that a short pointed end could be pinned against the otic process of the quadrate bone (Baumel et al., 1993), which lies within the anterior part of the opening that also admits entrance to the external acoustic meatus. This enabled the head to be held firmly in a position that conformed with demands of the stereotaxic atlas of the zebra finch brain (Konishi, unpublished) that places the confluence of mid-sagittal and

cerebellar sinuses (the 'Y' sinus) 0.3 mm caudal to inter-aural zero. An advantage of this positioning is that the external acoustic meatus remains open for the reception of auditory stimuli, while the head remains firmly held with 'ear bars'. Upwards mobility of the upper beak was restricted with a piece of clay anchored to the beak bar. The head was angled downwards at an angle of 45 degrees to the horizontal, as for a similar sized species (canary; Stokes et al., 1974).

Evocation of visual responses and deposition of neural tracers

Recordings of visually evoked, extracellular responses in the pons (PL), thalamus (Uva/rUva) and nidopallium (NI) were made using low impedance (2-4 M Ω) tungsten microelectrodes (FHC, Bowdoin, ME, USA) carried in the arm of a David Kopf electronically controlled hydraulic micropositioner (Model 2650). An A-M Systems differential amplifier, Model 1800, amplified and band-pass filtered the neural signals between 300 Hz and 5 KHz, with the reference being attached to the head skin. Neural signals were also monitored with a loud speaker and a digital oscilloscope. They were also fed to a computer running Scope 3 software and to a MacLab 8/30 A-D (ADInstruments), which was triggered once per second by a TTL pulse that also drove a white LED placed 1 cm from the contralateral eye. The LED had a rise time of only a few milliseconds, but had a decay time of about 100 milliseconds. Once reliable visual responses could be evoked at a particular locus, auditory stimuli in the form of hand claps, whistles, clicks, and human voice, and somatosensory stimuli supplied by brush strokes and pulses of air to the feathers over many different parts of the body, were used to assess the exclusiveness of the visual responses. This assessment also included electronically timed auditory and somatosensory stimuli: the TTL pulse that drove the flash stimulus was used instead

to trigger a picospritzer (General Valve) that supplied 30 msec pulses of air at 20 psi directed via a narrow flexible tube to various parts of the body. The picospritzer valve, which was positioned near the bird, also supplied an auditory stimulus in the form of a loud click at each pulse.

The stereotaxic coordinates of visual responses were then used either in the same bird or different birds to guide glass micropipettes to visually responsive loci for the recording and deposition of neural tracers. The glass micropipette (WPI, 1.5 mm outside diameter) were pulled in a David Kopf vertical puller (Model 700C) and broken back to produce tips of between 12 and 20 microns internal diameter. These were filled with either biotinylated dextran amine (BDA, Molecular Probes, either 10,000 or 3,000 molecular weight, 10% in phosphate buffered saline (PBS)) or cholera toxin B-chain (cholera toxin B-subunit; List Laboratories, Campbell, CA, 1% in PBS). Visually evoked recordings were made through the injection pipette to verify placement, and then the recording leads were replaced by leads from a high voltage current source (Midgard) to make iontophoretic injections, using either 4 μ A for BDA or 2 μ A for CTB, 7 seconds on, 7 seconds off, for a total of 15-20 minutes.

The pipette was then withdrawn, the head skin glued together with tissue adhesive (3M Vetbond), and the bird placed in a warmed recovery cubicle until fully conscious (3-6 hours). Survival time was 3-4 days.

Histology

Birds were deeply anesthetised with an intramuscular injection overdose of ketamine/xylazine and perfused transcardially with 50 ml normal saline followed by 150 ml of 4% paraformaldehyde (PFA) in phosphate buffer, pH 7.4. The calvarium was removed and the brain postfixed for 3-5 hours. It was then blocked in the

stereotaxic plane, removed from the skull, and equilibrated in 30% sucrose buffer until it sank. Frozen sections (35 microns) were cut with a Microm sliding microtome and collected serially and alternately in two 24-well trays.

To visualize BDA, sections were washed 3x10 minutes in PBS, bleached for 20 minutes in 50% aqueous methanol containing 1% hydrogen peroxide and then incubated for 1 hour in streptavidin-horseradish peroxidase (HRP) conjugate (Invitrogen), 1:1,000 in 0.4% PBS-Triton X-100, washed 3x10 minutes in PBS, and treated with 0.025% 3,3-diaminobenzidine (DAB) in PBS containing 0.015% cobalt chloride to produce a black reaction product. To visualize CTB, sections were incubated in a goat anti-CTB antibody (List Laboratories, Campbell, CA; RRID: AB_10013220) at 1:33,000 final dilution in 0.4% PBS-Triton X-100 and 2.5% normal rabbit serum. The CTB antibody was raised against purified cholera toxin and does not result in labeling following preabsorption of the antibody with excess concentration of cholera toxin (Stocker et al., 2006), and no labeling is seen in material in which a CTB injection has not been performed (Kubke et al., 2004). Sections were then incubated for 1 hour in a biotinylated rabbit anti-goat secondary antibody (Sigma-Aldrich, St. Louis, MO) 1:300 in PBS-Triton X-100, washed 3x10 minutes in PBS, and incubated for a further hour in streptavidin-HRP at 1:1,000 in PBS. Sections were then treated with the DAB mixture without cobalt chloride, which yielded a brown reaction product. Sections were mounted on subbed slides, dehydrated in a graded alcohol series, and coverslipped with DPX (Scharlau, Spain). Chosen sections were counterstained with Neutral Red, and labeled projections were drawn using a drawing tube and scanned into a computer. Sections were also viewed in a Nikon 80i Eclipse microscope and photographed with a 5 megapixel camera. Images were adjusted for brightness and contrast using Adobe PhotoShop and labeled

and assembled for publication using Adobe Illustrator.

RESULTS

Recordings of visually evoked neural responses

Figure 1 displays Scope records from the ventrolateral pons (PL), the posterior thalamus (rUva), and the intermediate nidopallium (NI). Satisfactory averaging of the responses by the Scope software (evoked at once per second for 50 flash presentations) was not always possible to achieve, indicating substantial temporal dispersion. When averaging was not possible, the response to a single stimulus presentation is shown as representative of similar responses to 10 successive stimulus presentations. Evoked visual responses in PL had stereotaxic coordinates, in millimetres, of P0.2-0.3, L1.5-1.6, and D6.5-6.8. Their latencies varied between ~60 and 80 msec and the responses were often distributed over most of the duration of the light flash (~100 msec), sometimes with an off-response coinciding with the end of the LED decay period.

Stereotaxic coordinates for recordings of visual responses in the posterior thalamus were A0.2-A0.35, L1.5-1.7, and D4.4-4.6. Responses were similar to those from PL, but were not as robust as those that can be recorded from nucleus rotundus, and again were temporally dispersed.

Coordinates for visual responses in NI ranged from A1.1-1.7, L2.6-3.5, and D1.6-3.1, depending on laterality: the more lateral and anterior the penetration, the more likely the electrode was to reach the entopallium below ~D3.0. This was indicated by a marked change in the extended duration and more robust nature of the evoked response. No attempt was made to sample the entire possible distribution of flash-evoked responses from the intermediate nidopallium. Rather, in reciprocal

fashion, recordings were concentrated in regions defined by the projections of Uva and rUva.

Within the various regions recorded from and finally injected with tracer, there were no responses to either auditory and/or somatosensory stimuli, i.e., tracer injections were made at sites responding only to the visual stimuli (see Methods and Materials). That the auditory stimuli were potentially effective in driving auditory evoked responses was indicated by the fact that, during the course of parallel, ongoing studies in this laboratory of the thalamic auditory nucleus ovoidalis and its telencephalic-recipient Field L, robust and highly sensitive responses could be recorded using the same auditory stimulus and recording procedures as those used in the present study.

Ascending anterograde labeling from PL injections

Figure 2A shows the location of one of four similar iontophoretic injections of BDA 3K into PL, and the predominantly ipsilateral projections to the thalamus are depicted as camera lucida drawings of chosen sections, with selected correlated photomicrographs. Labeled fibres from the injection site extended dorsolaterally on either side of the nucleus semilunaris (SLu; Fig. 2a1) and the parvocellular and magnocellular isthmic nuclei (Ipc and Imc). They then turned around the lateral corner of the tectal ventricle to enter the deep fibrous layer of the tectum. These labeled fibres proceeded dorsally around the full extent of the curve of the tectum to enter Uva from a lateral direction. Terminations partly surrounded Uva laterally and dorsally, but left unlabeled the core of the nucleus - which receives its predominant input from the pulmonary input-related ventrolateral brainstem (Reinke and Wild, 1998; Wild, 2004; 2008; Schmidt and Wild, 2014) (Fig. 2a2). At the level of the

rostral part of the medial spiriform nucleus (SpM) the rostral pole of Uva was completely labeled (Fig. 2b), after which fibres and terminations extended farther rostrally to occupy positions lateral, dorsolateral and ventral to the caudal pole of nucleus ovoidalis (Ov) (Fig. 2c). Dense terminal fields finally occupied similar positions at mid rostro-caudal levels of Ov, with more diffuse labeling surrounding Ov itself. There were no terminations in nucleus rotundus (Rt, including the triangular subnucleus, T) or the pretectal nuclei. The region between Uva, where it is usually depicted as grape-shaped (Nottebohm et al., 1982; Wild, 1994), and Ov, is not defined in traditional atlases of the avian brain, but the region can be visualized in transverse sections 80-82 of zebra finch brain #0821 in the zebra finch digital brain atlas (<http://zebrafinch.brainarchitecture.org/>), with the caudal pole of nucleus rotundus first making its appearance in section 82. Here we simply refer to the region rostral to Uva that receives the PL projections as rUva, identifying it as a rostral extension of the traditional grape-shaped Uva (see Discussion). At more rostral levels still, fiber and terminal labeling and scattered retrogradely labeled neurons occupied a vertically oriented tract running between the tractus ovoidalis (TOv) and Rt (Fig. 2d). Even more rostrally (but still caudal to the anterior commissure) some labeled fibers extended dorsolaterally through the thalamus to enter the subpallium where they formed a diffuse terminal field throughout the subpallial amygdala (SpA; Fig. 2e).

Retrograde labeling in the tectum and PL following injections in rUva

BDA and CTB injections in the thalamus produced similar patterns of retrograde labeling in the tectum and in PL, but because CTB injections tended to produce many more retrogradely labeled neurons than BDA injections, we illustrate the distribution of labeled neurons produced by a representative CTB injection (Fig.

3A). The center of this injection was located between the lateral border of caudal nucleus ovoidalis (Ov) and the rostral pole of Uva, i.e., in rUva. The cytoarchitecture of this previously undescribed region is shown in figure 3B, in which the nucleus labeled rUva is considered a rostral extension of nucleus uvaeformis (Uva: Wild, 1994) - see below. However, there was evidence of diffusion of tracer from the center of this injection, and others like it, to some adjacent structures, although there was tendency of this diffusion to respect the capsular borders of nuclei such as Ov and the annulus of the pretectal nucleus (PT). Regardless, the possibility of some uptake of tracer from areas of diffusion cannot be ruled out.

Retrogradely labeled neurons were located in several laminae of the ipsilateral tectum, predominantly in lamina 13, but also in 8-12 and 15. An occasional cell was found in 5b and even one cell in lamina 4. Labeled neurons were distributed throughout all rostrocaudal levels of the tectum (e.g., Fig. 3C), but in the contralateral tectum labeled neurons were almost totally confined to lamina 13 (Fig. 3D). Figure 3D also shows anterograde labeling in rUva on the contralateral side, reflecting the principal region of tracer uptake at the site of injection. Also, since no neurons were retrogradely labeled in the contralateral rUva, the anterograde labeling there was assumed to have arisen from tectal neurons that project to rUva bilaterally via branched axons (see Discussion). Labeled neurons were also found in the subtectum and nucleus intercollicularis (ICo), and in the nucleus lentiformis mesencephali (LM), which is known to project to DLL (Pakan et al., 2006), situated dorsal to the site of the injection. At the level of the injection, labeled neurons formed a distinct caudoventral cluster, laterally adjacent to the nucleus of the basal optic root (nBOR, Fig. 4A). A few labeled neurons were found in the ipsilateral superior vestibular and lateral cerebellar nuclei.

BDA injections in rUva were more confined to the nucleus (e.g., Fig. 8A) and although they labeled many fewer lamina 13 tectal neurons - probably at least partly due to the nature of the tracer itself (Reiner et al., 2000) - the pattern of retrograde labeling in the tectum was similar to that following CTB injections in rUva. An intriguing aspect of the BDA labeling was that, because of their relative sparseness, single labeled neurons in several sections could be seen to be rather evenly spaced by 400-500 microns throughout the entire curve of layer 13.

The same injections that produced retrograde labeling in the tectum also produced retrogradely labeled neurons predominantly, but not exclusively, in an external layer of the ipsilateral lateral pontine nucleus (LP; Fig. 3E, F) lying close to the ventrolateral border of the section. They also produced abundant anterograde fiber and terminal labeling in an internal, cell-dense layer of LP, in which there were embedded some neurons retrogradely labeled from rUva (Fig. 3E). However, it is unlikely that these anterograde projections originate from the injection site, (a) because LP injections did not retrogradely label neurons in Uva/rUva (see below) and (b) tectal injections anterogradely labeled both Uva/rUva and LP, possibly via branched axons (see below). CTB but not BDA injections in rUva also labeled neurons in the reticular formation overlying PL (Fig. 3E)

Retrograde labeling from PL injections

Tectum. The PL injections produced extensive retrograde labeling of neurons throughout the same deep tectal laminae (8-15) as did the rUva injections. There was even an occasional labeled neuron in the monolaminar 6 (Fig. 4). Neurons retrogradely labeled from PL injections were present throughout all regions of the tectum (dorsal, lateral, ventral, caudal, and rostral) without apparent differential

density. As described by Gamlin and Cohen (1986) for DLPc projecting neurons in the pigeon tectum, the soma size and dendritic direction and arborisation of labeled tectal neurons varied considerably, largely depending on which lamina the soma was in. Some dendrites extended laterally within the same or adjacent lamina as their soma, some extended in several directions, and some had radially oriented dendrites that reached the outermost retino-recipient layers. However, the axonal trajectory of individual tectal neurons could not be determined with certainty. It is possible that some tectal neurons project to PL via single, unbranched axons, but others could project to both PL and Uva/rUva via branched axons. Indeed, the same deep fibrous tectal lamina could carry the axons of both tectal and PL neurons projecting to the posterior thalamus, and/or tectal neurons projecting to the posterior thalamus and PL via branched axons. That the last was a real possibility was suggested by the fact that PL injections did not retrogradely label neurons in Uva/rUva; thus the anterograde labeling in the internal layer of PL could have resulted from somatopetal and somatofugal labeling of tectal neurons that project upon both Uva/rUva and PL via branched axons.

Forebrain. The tract situated between TOv and Rt, which was anterogradely labeled by PL injections (Fig. 2d), also contained scattered retrogradely labeled neurons, as well as at the base of this tract, immediately dorsolateral to the nucleus of the basal optic root (nBOR; Fig. 4G). The only other group of retrogradely labeled neurons found in the forebrain following PL injections was in the center of the arcopallium intermedium (AI, Fig. 4H).

Tectal neurons projecting to both Uva/rUva and PL?

The possibility that single tectal neurons project upon both PL and Uva/rUva was tested in 10 cases by making dual injections of tracers, one into rostral Uva and another into PL in the same bird: CTB Alexa 555 was injected into one and CTB Alexa 488 into the other. In 2 pressure injection cases these procedures produced enough retrogradely labeled tectal neurons to assess realistically the possibility of double labeling. Some of these neurons fluoresced green, some red, and many appeared yellow, i.e., were apparently double labeled. However, in both cases there was inadvertent contamination of the Uva/rUva site by spread/leakage of tracer from the PL site up the injection pipette, thereby precluding an unequivocal conclusion that some tectal neurons project to both Uva/rUva and PL via branched axons.

Contrary to a previous report in pigeons (Clarke, 1977; see also Gamlin and Cohen, 1988; Pakan et al., 2006), we found very little evidence in zebra finches that nuclei lentiformis mesencephali project upon PL. In the case depicted in figure 3, for instance, there were only 3 retrogradely labeled neurons in LM in one section of the entire brain.

Tectal projections to rUva and other thalamic nuclei

Tectal projections to Uva were described in zebra finches and other finches in a previous study (Wild, 1994), but additional injections were made into the tectum of 5 zebra finches in the present study to re-examine projections to the posterior thalamus and to verify projections to PL. The results of a large tectal injection of CTB are presented for illustrative purposes (Fig. 5): the injection was made through the lateral aspect of the stratum opticum, and covered the outer dozen tectal laminae, retrogradely labeling neurons throughout an extensive region of lamina 13. Ascending anterograde axonal labeling from this injection would therefore be expected to arise

from many of these lamina 13 neurons via intratectal somatopetal and somatofugal transport (Karten et al., 1997; Luksch et al., 1998), and possibly directly from neurons in more superficial laminae (Hunt and Künzle, 1976). Confirming our previous results in songbirds (Wild, 1994), Uva received a substantial tectal projection, except for its caudal core (Fig. 5B), and fiber and terminal labeling extended rostrally throughout rUva, similar to the pattern of labeling produced by PL injections (Fig. 5C). More rostrally there was massive, predominantly ipsilateral, anterograde labeling of Rt, the PT annulus (neurons in the center of which were retrogradely labeled from tectal layer 5b: Gamlin et al., 1996) and other thalamic nuclei (Fig. 5A), as expected on the basis of previous studies (Benowitz and Karten, 1976; Hunt and Künzle, 1976; Bischof and Niemann, 1990; Korzeniewska and Güntükün, 1990; Wild, 1994). There was also anterograde labeling of the internal layer of PL (Fig. 5D), suggesting that the similar labeling resulting from rUva injections (see above) could have originated from tectal neurons projecting to both rUva and PL. In a case that received a small BDA injection confined to the dorsal tectum, anterograde labeling in Uva was confined to its lateral and dorsal regions (not shown), reproducing in part the results of tectal and PL injections. In yet another case CTB was injected in the caudal tectum, and again the results were similar to those described above. Noteworthy was the absence in each case of terminations in the caudal core of Uva.

Descending projections identified by injections in PL

Labeled fibers produced by PL injections that proceeded caudally took one of two trajectories. One traveled ventrolaterally as a narrow tract throughout the periphery of the ipsilateral brainstem. *En route* terminal fields and several retrogradely labeled neurons were associated with this tract, especially at caudal

pontine levels (Fig. 6A). A few remaining fibers entered the ventral funiculus of the upper cervical spinal cord (Fig. 6B), but the specific origin of the tract was not verified retrogradely in the present study.

A separate tract passed from the injection site directly into the most dorsal aspect of the spinal lemniscus and proceeded caudally to pontine levels. Labeled fibers in the tract then entered the ipsilateral cerebellar peduncle on its most lateral aspect (Fig. 6C) and ascended, with some crossing to the opposite side within the white matter of the cerebellum and some remaining on the same side. The fibers terminated bilaterally in folia VII-IX as mossy fibre parallel bands (Fig. 6D), as shown by Clarke (1977) in pigeons on the basis of injections of tritiated proline into PL.

Large air pressure injections of CTB were made into caudal cerebellar folia in 3 birds to verify the origin of these projections in PL. Numerous retrogradely labeled neurons were found in PL (Fig. 6E). To determine whether the neurons that projected to the cerebellum were the same as or separate from those that project to Uva and rostral Uva, injections of different fluorescent CTB tracers were made into caudal cerebellar folia and rostral Uva. The results showed that, although there was some admixture of cells projecting to rUva and the cerebellum, those projecting to rUva tended to lie ventral to those projecting to the cerebellum (Fig. 6F), and no double labeled neurons were observed. Furthermore, neurons retrogradely labeled from cerebellar injections, but not those retrogradely labeled from Uva/rUva injections, were enmeshed in fibre and terminal labeling, presumably originating from tectal neurons.

Projections from Uva/rUva to the nidopallium

The injections in Uva/rUva also produced extensive anterograde labeling of ascending fibres that terminated densely in different regions of the ipsilateral intermediate nidopallium (Figs. 7 and 8B). As the injection site was moved from Uva through rUva in different cases, the terminal field in NI shifted gradually from caudomedial to rostromedial, until it approximated the medial corner of the entopallium (Fig. 7H). The densest part of the terminal field in each case was immediately dorsal to the pallial-subpallial border (Fig. 8B), but less dense anterograde labeling also extended dorsolaterally throughout the depth of the nidopallium. Some fibers even penetrated the mesopallial border (LaM) to terminate sparsely in the ventral mesopallium (see also Fig. 7 in Wild, 1994), but no projections from rUva to HVC or the caudolateral nidopallium were observed.

On the basis of recordings of visually evoked multiunit responses, injections of BDA or CTB were made into various regions of the intermediate nidopallium between the entopallium rostromedially and nucleus interface (NIf) caudomedially, in order to validate the anterograde projections described above. Two injections located rostromedially in NI, one of BDA (Fig. 8C) and the other of CTB (Fig. 8E), were located medially adjacent to the entopallium. These injections retrogradely labeled neurons in rUva, where they were located lateral, dorsolateral and ventrolateral to Ov (Fig. 8D, F), mirroring the pattern of terminations of PL projections to this region. This pattern was amply confirmed by another, large CTB injection centered slightly more medially in NI, which retrogradely labeled a host of neurons in rUva that were completely overlapped by the distribution of anterograde fiber and terminal labeling produced by an injection of BDA into PL in the same bird (Fig. 2c). Injections that were centered more medially in NI, including NIf, retrogradely labeled neurons in different parts of Uva (see Wild, 1994). None of the injections in NI, including those

adjacent to the entopallium, produced retrograde labeling in nucleus rotundus (Rt).

Anterograde labeling from NI injections

Anterograde labeling produced by injections in the intermediate nidopallium was located in two separate regions. One was in the mesopallium dorsolateral to LaM (Fig. 8G) and another was in the lateral striatum (LSt; Fig. 8H) ventromedial to the injection in NI. BDA injections in NI showed that the location of the terminal labeling in the mesopallium included the ventral location of the relatively sparse terminal labeling in the mesopallium produced by rUva injections; but they also showed that terminal labeling was also present more dorsally and medially in the mesopallium. Any anterograde, terminal labeling in the mesopallium from CTB injections in NI, however, was impossible to distinguish from the masses of retrogradely labeled cells that populated the ventral part of the mesopallium, adjacent to LaM (Fig. 8D), indicating reciprocal nidopallial-mesopallial connections.

Anterograde labeling in the LSt produced by NI injections (Fig. 8D, H) was bounded laterally by that part of LSt that receives projections from the entopallium (Krütfeldt and Wild, 2004).

Figure 9 provides schematic summaries of the various inputs to Uva and rUva and the first and second tectofugal pathways..

DISCUSSION

Since the naming of Uva (proper name *uvaeformis* = grape shaped) in a songbird (Nottebohm et al., 1982), the nucleus has generally been regarded as a dedicated component of the song system. However, the similarity of Uva to DLPC in a non-songbird (pigeon), in terms of its position in the caudal thalamus, its relation to

the habenular-infundibular tract, its cell types, its afferent and efferent projections, and its lack of sexual dimorphism (Wild, 1994), together question this dedication. In pigeons ‘DLPr’ was used by Gamlin and Cohen (1986) to describe a nucleus lying immediately rostral to DLPc, and in parallel fashion we have given the name rUva to the rostral extension of Uva in the zebra finch. However, Gamlin and Cohen’s (1986) division of DLP in pigeons into caudal and rostral parts was not supported by other studies of single unit recordings of responses to visual, auditory and somatosensory stimuli made throughout the full rostrocaudal extent of the nucleus (Korzeniewska, 1987; Korzeniewska and Güntürkün, 1990). These authors suggested, instead, that DLP was polymodal, with many cells responding to combinations of two or even three types of stimuli. Similar single unit recordings have not been made in either Uva or rUva, but the variety of inputs to Uva and multiunit recordings from the nucleus suggest that it is also multimodal. In contrast, in the present study only visual, and not auditory or somatosensory, multiunit responses were recorded from rUva, thereby suggesting it is in this respect different from both Uva/DLPc and DLPr.

Although Uva is undeniably multimodal, like its proposed homolog DLPc in pigeons, it receives other projections that have thus far not been identified in non-songbirds (indeed, it would be very interesting if they were!) These originate from nucleus parambigualis (PAm) in the ventrolateral medulla, a nucleus that forms part of the rostral ventral respiratory group and likely mediates information derived from the lung and possibly air sacs by way of the vagus nerve and nucleus tractus solitarius (Reinke and Wild, 1998; Striedter and Vu, 1998; Wild, 2004; 2008; Schmidt and Wild, 2014). The PAm inputs to Uva appear to be quite specific, in that they are concentrated in a caudal core of the nucleus, a core that seems to be relatively free from inputs from other sources (present and previous results), and to preferentially

project to HVC (Wild, unpublished observations). The pulmonary-related inputs from PAm, and the auditory inputs to Uva from LLV seem to ‘make functional sense’ within the context of Uva regarded as a key nucleus in the song control system, but the somatosensory and visual inputs are not so readily incorporated into this schema. In so far as such inputs arise from either Uva or Nif, which have direct or indirect access to HVC, it is not difficult to imagine that they also could play a role in vocal control, perhaps in relation to visual displays associated with song. In contrast, the visual rUva and NI regions defined in the present study do not appear to be directly related to the song control system, and likely contribute significantly to other behaviours in the visual realm.

The present study has confirmed previously described tectal projections to Uva (Wild, 1994) and shown that similar projections extend more rostrally throughout rUva. Since it is known that neurons in lamina 13 of the tectum (the tectal ganglion cells, or TGC’s, of Ramón y Cajal, 1911) are the major source of projections to both nucleus rotundus (Rt) of the first tectofugal system and Uva/rUva of the second tectofugal system, it is of interest to determine if they are the same neurons that project to both. We tentatively suggest that they are not, based on the fact that although injections in rUva resulted in anterograde labeling of the contralateral rUva – via somatopetal and somatofugal transport of tectal neurons that project bilaterally via branched axons – the same injections did not produce anterograde labeling in either the ipsilateral or the contralateral Rt, which they would have done had the same layer 13 tectal neurons projected to both Rt and rUva. (It is known that single neurons in lamina 13 project to Rt bilaterally, at least in chicks (Deng and Rogers, 1998a) and pigeons (Karten et al., 1997; Marin et al., 2003; see also Bischof and Niemann, 1990; Hunt and Künzle, 1976; Wild, 1994; Deng and Rogers, 1998b). Nevertheless, double

retrograde labeling of tectal neurons from injections of differently colored tracers into rUva and Rt are required to answer this question unequivocally.

Whether visual input to rUva also derives from the lateral pontine nucleus (PL) cannot be answered with certainty from the present results. Some PL neurons retrogradely labeled from rUva injections were embedded within the anterograde labeling produced by the same rUva injections, labeling suspected to ultimately derived from tectal neurons; but some were located deep to the anterograde labeling. It seems possible, therefore, that some PL neurons could provide tectally derived visual input to rUva, but that most PL neurons are concerned with providing visual input to the caudal cerebellum.

PL is located in the ventrolateral pons such that its caudal border is only a couple of hundred microns rostral and lateral to the rostral border of auditory LLV, which has also been shown to project upon Uva (Coleman et al., 2007). With this in mind, we took pains to determine that our tracers were injected only at visually and not at auditory responsive loci. However, our injections in PL could well have interrupted LLV efferents that also course dorsolaterally, in this case to terminate extremely densely in the avian inferior colliculus, known in birds as nucleus mesencephalicus lateralis, pars dorsalis (MLd) (Wild et al., 2010). Notwithstanding these considerations, no labeled fibres or terminations were observed in MLd as a result of our PL injections, suggesting that uptake of tracer was at least primarily from visual PL neurons. These neurons had axons that circumnavigated the tectal ventricle before terminating in Uva and rUva.

Within rostral Uva, labeled fibres and terminations first occupied a region dorsal to the medial spiriform nucleus, as shown by Wild (1994, Fig. 8). Within rUva they then gradually approximated the caudal pole of nucleus ovoidalis (Ov). Finally

they surrounded Ov on its lateral, dorsolateral and ventral aspects at mid-rostrocaudal levels of Ov. The caudal pole of nucleus rotundus (Rt) and its triangular subdivision (T; Laverghetta and Shimizu, 2003) begin to appear ventrolateral to these rostral terminations, but we believe that they receive no terminations from PL (see Fig. 2Dd, E). Moreover, rUva injections did not anterogradely label any part of the entopallium, whereas T can be retrogradely labeled from all parts of the entopallium (Laverghetta and Shimizu, 2003; Fredes et al., 2010). Finally, T was not retrogradely labeled from any of the injections in NI made in the present study. Thus, rUva and T appear to be separate visual nuclei, albeit in proximity, with rUva lying caudal to T.

In pigeons a nucleus semilunaris parovoidalis (SPo) occupies a position ventrolaterally adjacent to Ov (Karten and Hodos, 1967) and receives auditory input from two of the three nuclei of the lateral lemniscus (LLV and LLD: Wild, 1987b). Despite its somewhat similar position with respect to Ov, however, SPo in pigeons seems unlikely to be homologous to the regions receiving PL and tectal projections in the zebra finch because: a) these regions in the zebra finch are separated from Ov by a gap, whereas SPo in pigeons is adjacent to Ov; b) they receive visual rather than auditory inputs; and c) their output is to the visually responsive nidopallium, not to L2b of the thalamorecipient auditory field L (Wild et al., 1993). Furthermore, according to Vates et al. (1996), neurons that project upon L2b in zebra finches are located ventromedially within Ov itself, not in a nucleus ventrolateral to Ov, as in pigeons (Karten and Hodos, 1967).

The terminal fields of PL projections that surrounded Ov on its dorsolateral, lateral and ventrolateral aspects did not form a single homogeneous field. Although this could suggest more than a single source of input, the pattern of anterograde labeling was strikingly replicated by the pattern of retrograde labeling produced by a

single BDA injection placed medially adjacent to the entopallium NI (Fig. 8). It is interesting to note, also, that the patch of terminal labeling dorsolateral to Ov would probably lie immediately caudal to the somatosensory nucleus DIVA (Wild, 1987a; 1997), thereby indicating a functional topography of tecto-visual and somatosensory projections to the dorsal thalamus.

Projections to caudal thalamic regions between Rt and TOv are puzzling, as are the retrogradely labeled neurons within this region. We have not attempted to determine the source(s) of the afferents using retrograde labeling techniques, so we do not know whether both the tectum and PL innervate this region. The tract-like nature of the afferentation resembles the input to Ov that traverses the adjacent TOv, and it is possible that these afferents provide some of the input to rUva. The diffuse projections to the subpallial amygdala are also curious and equally enigmatic.

Functional topography of Uva and rUva projections to the nidopallium

Gamlin and Cohen (1986) in pigeons discussed the possibility that projections to more rostral nidopallial regions medially adjacent to the entopallium, that derived from a thalamic nucleus (DLPr) rostrally extensive with DLPc, were somatosensory. However, both Wild (1987a) and Funke (1989) found in pigeons that the principal somatosensory thalamic locus was not DLP, but nucleus dorsalis intermedialis ventralis anterior (DIVA), located ventral to DLP and dorsolateral to nucleus ovoidalis. DIVA projects, not to the nidopallium, but to the rostral Wulst (Wild, 1987a; 1997; Funke, 1989; see also Wild et al., 2008). The strongly somatosensory-responsive region in the nidopallium in pigeons is the major DLPc projection field (Wild, 1987a; Funke, 1989), but visual responses can also be found there (Wild, 1994), as would be expected from the presence of visually responsive units in DLPc (Gamlin and Cohen,

1986). In finches, similarly robust somatosensory and visual responses can be recorded in NIf, which occupies a very similar position in the nidopallium to that of the major DLPc projection field in pigeons (Wild, 1994). It thus appears that NIf, like Uva from which it derives its thalamic input, and like its equivalent nidopallial field in pigeons, is multifunctional, despite its being generally regarded as an auditory nucleus (Lewandowski et al., 2013). In contrast, the NI region between NIf and the entopallium, which is innervated by rUva, seems at least predominantly visual in nature, although single unit studies are required to assess the possibility of responses to other kinds of stimuli.

Within the intermediate nidopallium terminal fields from rUva injections together occupied a large, visually responsive region between the entopallium laterally and NIf medially. That these projections are probably topographic was indicated by the fact that the rostrally located rUva injections produced terminal fields in NI medially adjacent to the dorsomedial corner of the entopallium, whereas injections located slightly more caudally and that included the rostral pole of Uva, produced terminal fields that occupied more caudal and medial parts of the nidopallium. Injections confined to the traditional grape-shaped, caudal Uva, produce terminal fields in NIf, which is the most medial component of the Uva/rUva projection fields in NI (Wild, 1994).

Further indications of functional topography are provided by the results of injections confined to the dorsomedial corner of the entopallium in zebra finches, which retrogradely label neurons in the dorsomedial corner of nucleus rotundus (Wild, unpublished observations; see also Laverghetto and Shimizu, 2003 and Krützfeldt and Wild, 2004 for complementary results of rotundal injections). These retrogradely labeled rotundal neurons lie in proximity to those in rUva retrogradely

labeled from nidopallial injections medially adjacent to the entopallium (Wild, 1994 and present study), suggesting a clear topography of visual projections from these two otherwise separate tectofugal pathways.

rUva projections to the mesopallium

Within the context of the song control circuitry, Akutagawa and Konishi (2010) showed that Uva projections to NIf also crossed the mesopallial lamina to terminate in nucleus Avalanche, which was previously shown to be innervated by HVC (Nottebohm et al., 1982). In addition, NIf was also shown to project upon Avalanche and to receive a projection from Avalanche. Somewhat similarly in the present study, rUva projections to NI were also found to cross the mesopallial lamina and to terminate in the ventral mesopallium, and that this mesopallial region probably projects back upon NI. However, the rUva projections to the mesopallium seem to be meagre compared with the Uva projections to Avalanche, and also meagre compared with the distribution of NI projections to the mesopallium. Nevertheless, the similarity in the pattern of projections to NIf and NI from Uva and rUva, respectively, is noteworthy.

Nidopallial projections to the lateral striatum

In the present study nidopallial injections produced anterograde labeling not only in the mesopallium but also in the lateral striatum. Specifically, two nidopallial injections located adjacent to the dorsomedial corner of the entopallium both produced anterograde labeling of the lateral striatum adjacent to that produced by entopallial injections (Krütfeldt and Wild, 2004; 2005; Alpar and Tömböl, 2000), while those located more medially in the nidopallium produced terminal fields more

medially in the striatum. These findings imply that a large part of the lateral striatum at these rostrocaudal levels could be the source of both direct and indirect (via the pallidum) extratelencephalic outputs from two major tectofugal visual systems. These specific outputs from the striatum are clearly a major potential source of visual projections to sub-telencephalic targets, in addition to those more usually promulgated from the arcopallium (Shimizu and Bowers 1999).

PL projections to the cerebellum

PL projections to the cerebellum were described in chicks by Brodal et al. (1950), in pigeons by Clarke (1977), and in zebra finches by the present study. Clarke (1977) interpreted these visuomotor projections in the context of the accessory optic system, because of the afferents to PL from the ventral part of the retinorecipient nucleus lentiformis mesencephali (LM). Our present study in zebra finches failed to show a robust projection from LM to PL, which could be a function of the specific locus of our injections in the more rostradorsal parts of PL. Comparisons with the location of Clarke's injections is also complicated by his sole use of sagittal sections. In the present study the cerebellar-projecting neurons in PL were enmeshed in anterograde fiber and terminal labeling resulting from rUva or tectal injections (Fig. 6F), but our techniques did not permit a determination as to whether they were in direct receipt of these projections. Similarly for the rUva-projecting PL neurons that were embedded in the same anterograde labeling; Fig. 3E.

The ipsilateral tectal input to PL as shown in the present study is via the tectopontine tract. In pigeons this tract has been described as originating predominantly in dorsal parts of the tectum (Münzer and Wiener, 1898; Clarke, 1977; Reiner and Karten; 1982; Hellman et al., 2004), but this was not obviously the case in

zebra finches in the present study. Perhaps this reflects a difference in the relative functional importance of upper versus lower visual field representations in the tectum in different species (see Hellman et al., 2004), but it may also reflect the fact that in the present study the retrograde labeling in the tectum was produced by iontophoretic PL injections that were largely confined to the nucleus, rather than by large pressure injections of tracer that covered much of the lateral tectum.

Comparative and functional considerations

Gamlin and Cohen (1986) noted distinct similarities between the second tectofugal projection system in pigeons and certain tectothalamic and thalamocortical visual projections in reptiles and mammals. Specifically, they likened DLPc to a part of the posterior dorsal thalamic group (PO) of mammals, namely the suprageniculate nucleus (SG), and noted the visual nature of its cells in cats and their projections to visual areas of the cortex. While our findings regarding the second tectofugal system in the zebra finch are similar in many respects to those described in pigeons, the complex issues surrounding the homologous relationship of posterior thalamic nuclear groups and their projections in reptiles, birds and mammals (Guirado et al., 2005) preclude a categorical statement as to the comparative identity of Uva/rUva and their pallial projections. Moreover, there is little information on the function of the second tectofugal pathway in birds. Sensory or visual discrimination deficits following lesions of DLP have not been found (Güntürkün, 1997; Hartmann and Güntürkün, 1998). There is some suggestion that the nidopallial region medially adjacent to the entopallium is involved in processing low-spatial frequency visual information (Hodos et al., 1986), but whether the input to this region constitutes a visual stream separate from those to the entopallium is not known (Nguyen et al., 2004).

Güntürkün (1984) suggested the presence of a third visual system in pigeons, based on relatively short latency evoked responses in the caudolateral nidipallium. This is a different region from the rUva projection zone of the present study. Also, the thalamic inputs to the regions recorded from were not then determined, but these nidopallial regions appear to be different from those of the DLP projection field reported by Güntürkün and Kröner (1999).

Brodal et al. (1950) proposed that the avian PL would correspond to a pontine component of the cortico-pontine system in mammals (but see Wild and Williams, 2000a; b). However, projections to PL from either the visual or anterior Wulst have not been noted (Karten et al., 1973; Wild and Williams, 2000a). But in the present study a conspicuous group of retrogradely labeled cells in the cerebrum following injections in PL was located in the center of the intermediate arcopallium (Ai). Although the homologous status of the avian arcopallium is highly controversial (Striedter, 2005), its intermediate region has been suggested to contain many neurons similar to those of laminae 5/6 of mammalian cortex, by virtue of their descending projections and targets, and their gene expression (Karten, 1969; Zeier and Karten, 1971; Butler et al., 2011; Dugas-Ford et al., 2010). Whether the Ai neurons retrogradely labeled from PL injections in turn receive specific projections from visual parts of the hemisphere, perhaps originating specifically in nidopallial regions that receive rUva inputs, is currently unknown. However, a similar multisynaptic series of visual projections leaving the entopallium and terminating in the arcopallium was originally proposed by Ritchie (1979) and substantiated by Husband and Shimizu (1999; see also Shimizu and Bowers, 1999) in pigeons, although the subtelencephalic target of the Ai neurons was/is unknown.

Although our attempts to double label tectal output neurons were not

conclusive, the possibility that some tectal neurons have branched axons that innervate both Uva/rUva and PL, would contrast with previous findings of tectal neurons that have either an ascending or a descending axon, but not both (Reiner and Karten, 1982; Hellmann et al., 2004).

REFERENCES

- Akutagawa G, Konishi M. 2005. Connections of thalamic modulatory centers to the vocal control system of the zebra finch. *Proc Natl Acad Sci, USA* 102:14086-14091.
- Akutagawa G, Konishi M. 2010. New brain pathways found in the vocal control system of a songbird. *J Comp Neurol* 518:3086-3100.
- Alpar A, Tömböl T. 2000. Efferent connections of the ectostriatal core. An anterograde tracer study. *Anat Anz* 182:101–110.
- Baumel JJ, King AS, Breazile JE, Evans HE, Vanden Berge JC. 1993. *Handbook of Avian Anatomy: Nomina Anatomica Avium*. Publication of the Nuttall Ornithological Club.
- Benowitz LI, Karten HJ. 1976. Organization of the tectofugal visual pathway in the pigeon: a retrograde transport study. *J Comp Neurol* 167:503–520.
- Bischof H-J, Niemann J. 1990. Contralateral projections of the optic tectum in the zebra finch (*Taeniopygia guttata castonotis*). *Cell Tiss Res* 262:307-313.
- Brodal F, Kristiansen K, Jansen J. 1950. Experimental demonstration of a pontine homologue in birds. *J Comp Neurol* 92:23-69.
- Butler AB, Reiner A, Karten HJ. 2011. Evolution of the amniote pallium and the origins of mammalian neocortex. *Ann N Y Acad Sci* 1225:14–27.
- Clarke PGH. 1977. Some visual and other connections to the cerebellum of the pigeon. *J Comp Neurol* 174:535-552.
- Coleman MJ, Roy A, Wild JM, Mooney R. 2007. Thalamic gating of auditory responses in telencephalic song control nuclei. *J Neurosci* 27:10024–10036.
- Deng C, Rogers LJ. 1998a. Bilaterally projecting neurons in the two visual pathways of chicks. *Brain Res* 794:281-290.
- Deng C, Rogers LJ. 1998b. Organisation of the tectorotundal and SP/IPS-rotundal

- projections in chicks. *J Comp Neurol* 394:171-185.
- Dugas-Ford, Rowell JJ, Ragsdale CW. 2012. Cell-type homologies and the origins of the neocortex. *Proc Natl Acad Sci U.S.A.* 109:16974–16979.
- Engelage J, Bischof H-J. 1993. The organization of the tectofugal pathway in birds: a comparative review. In: Zeigler HP, Bischof H-J (Eds) *Vision, brain and behavior in birds*. Cambridge, MA: MIT Press, pp 137–158.
- Fortune ES, Margoliash D. 1995. Parallel pathways and convergence onto HVC and adjacent neostriatum in the adult zebra finch (*Taeniopygia guttata*). *J Comp Neurol* 325:388-404.
- Fredes F, Tapia S, Letelier JC, Marin G, Mpodozis J. 2010. Topographic arrangement of the rotundo-entopallial projection in the pigeon (*Columba livia*). *J Comp Neurol* 518:4342–4361.
- Funke, K. 1989. Somatosensory areas in the telencephalon of the pigeon. II Spinal pathways and afferent connections. *Exp Brain Res* 76:620-638.
- Gamlin PDR, Cohen DH. 1986. A second ascending visual pathway from the optic tectum to the telencephalon in the pigeon (*Columba livia*). *J Comp Neurol* 250:296-310.
- Gamlin PDR, Reiner A, Keyser KT, Brecha N, Karten HJ. 1996. Projection of nucleus pretectalis to a retinorecipient tectal layer in the pigeon (*Columba livia*). *J Comp Neurol* 368:424-438.
- Guirado S, Real A, Davila JC. 2005. The ascending tectofugal visual system in amniotes: new insights. *Brain Res Bull* 66:290-296.
- Güntürkün O. 1984. Evidence for a third primary visual area in the telencephalon of the pigeon. *Brain Res* 294:247-254.
- Güntürkün O. 1997. Cognitive impairments after lesions of the neostriatum

caudolaterale and its thalamic afferent in pigeons: functional similarities to the mammalian prefrontal system? *J Brain Res* 38:133-144.

Güntürkün O, Kröner S. 1999. A polysensory pathway to the forebrain of the pigeon: the ascending projections of the nucleus dorsolateralis posterior thalami (DLP). *Euro J Morphol* 37:185-189.

Hartmann B, Güntürkün O, 1998. Selective deficits in reversal learning after neostriatum caudolaterale lesions in pigeons: Possible behavioural equivalencies to the mammalian prefrontal system. *Behav Brain Res* 96:125-133.

Hellmann B, Güntürkün O, Manns M. 2004. Tectal mosaic: organization of the descending tectal projections in comparison to the ascending tectofugal pathway in the pigeon. *J Comp Neurol* 472:395-410.

Hodos W, Weiss SRB, Bessette BB. 1986. Size threshold changes after lesions of the visual telencephalon in pigeons. *Behav Brain Res* 21:203-214.

Hunt SP, Künzle H. 1976. Observations of the projections and intrinsic organization of the pigeon optic tectum: An autoradiographic study based on anterograde and retrograde, axonal and dendritic flow. *J Comp Neurol* 170:153-172.

Husband SA, Shimizu T. 1999. Efferent projections of the ectostriatum in the pigeon (*Columba livia*). *J Comp Neurol* 406:329–345.

Karten HJ. 1969. The organization of the avian telencephalon and some speculations on the phylogeny of the amniote telencephalon. *Ann NY Acad Sci* 167: 164–179.

Karten HJ, Revzin AM. 1966. The afferent connections of the nucleus rotundus in the pigeon. *Brain Res* 2:368–377.

Karten HJ, Hodos W. 1967. *A Stereotaxic Atlas of the Brain of the Pigeon (Columba livia)*. Johns Hopkins Press, Baltimore.

Karten HJ, Hodos W. 1970. Telencephalic projections of the nucleus rotundus in the

pigeon (*Columba livia*). *J Comp Neurol* 140:35-52.

Karten HJ, Hodos W, Nauta WJ, Revzin AM. 1973. Neural connections of the “visual Wulst” of the avian telencephalon. Experimental studies in the pigeon (*Columba livia*) and owl (*Speotyto cunicularia*). *J Comp Neurol* 150:253–278.

Karten HJ, Cox K, Mpodozis J. 1997. Two distinct populations of tectal neurons have unique connections within the retinotectorotundal pathway of the pigeon (*Columba livia*). *J Comp Neurol* 387:449–465.

Kitt CA, Brauth SE. 1982. A paleostriatal-thalamic-telencephalic path in pigeons. *Neuroscience* 11:2735-2751.

Korzeniewska E. 1987. Multisensory convergence in the thalamus of the pigeon (*Columba livia*). *Neurosci. Lett.* 80, 55–60.

Korzeniewska E, Güntürkün O. 1990. Sensory properties and afferents of the N. dorsolateralis posterior thalami of the pigeon. *J Comp Neurol* 292:457-479.

Krützfeldt NOE, Wild JM. 2004. Definition and connections of the entopallium in the zebra finch (*Taeniopygia guttata*). *J Comp Neurol* 468: 452–465.

Krützfeldt NOE, Wild JM. 2005. Definition and novel connections of the entopallium in the pigeon (*Columba livia*). *J Comp Neurol* 490:40–56.

Kubke MF, Ross, JR, Wild JM. 2004. Vagal innervation of the air sacs in a songbird, *Taeniopygia guttata*. *J Anat (Lond)* 204:283–292.

Laverghetto AV, Shimizu T. 2003. Organization of the ectostriatum based on afferent connections in the zebra finch (*Taeniopygia guttata*). *Brain Res* 963:101–112.

Lewandowski B, Vyssotski A, Hahnloser RHR, Schmidt MF. At the interface of the auditory and vocal motor systems. Nif and its role in vocal processing, production and learning. *J Physiol – Paris* 107:178-192.

Luksch H, Cox K, Karten HJ. 1998. Bottlebrush dendritic endings and large dendritic

fields: motion-detecting neurons in the tectofugal pathway. *J Comp Neurol* 396:399-414.

Marin G, Letelier JC, Henny P, Sentis E, Farfan G, Fredes T, Pohl N, Karten HJ, Mpodozis J. 2003. Spatial organization of the pigeon tectorotundal pathway: an interdigitating topographic arrangement. *J Comp Neurol* 458:361-380.

Münzer E, Wiener H. Beitrage Bur Anatomie und Physiologie des Centralnervensystems der Taube. *Monatschr. Psych. u. Neur.* 3: 379; cited in Brodal et al. (1950).

Nguyen AP, Spetch ML, Crowder NA, Winship IR, Hurd PL, Wylie DRW. 2004. A dissociation of motion and spatial-pattern vision in the avian telencephalon: Implications for the evolution of “visual streams”. *J Neurosci* 24:4962– 4970.

Nottebohm F, Kelley DB, Paton JA. 1982. Connections of vocal control nuclei in the canary telencephalon. *J Comp Neurol* 207:344–357

Pakan JMP, Krueger K, Kelcher E, Cooper S, Todd KG, Wylie DRW. 2006.

Projections of the nucleus lentiformis mesencephali in pigeons (*Columba livia*): a comparison of the morphology and distribution of neurons with different efferent projections. *J Comp Neurol* 495:84-99.

Ramón y Cajal S. 1911. *Histologie de systeme nerveaux de l’homme et de vertebres.* Paris: Maloine.

Reiner A, Karten HJ. 1982. Laminar distribution of the cells of origin of the descending tectofugal pathways in the pigeon (*Columba livia*). *J Comp Neurol* 204:165–187.

Reiner A, Veenman CL, Medina L, Jiao Y, Del Mar N, Honig MG. 2000. Pathway tracing using biotinylated dextral amine. *J Neurosci Meth* 103:23-37.

Reiner A, Perkel DJ, Bruce LL, Butler AB, Csillag A, Kuenzel W, Medina L,

Paxinos G, Shimizu T, Striedter G, Wild M, Ball GF, Durand S, Güntürkün O, Lee DW, Mello CV, Powers A, White SA, Hough G, Kubikova L, Smulders TV, Wada K, Dugas-Ford J, Husband S, Yamamoto K, Yu J, Siang C, Jarvis ED. 2004. Revised nomenclature for avian telencephalon and some related brainstem nuclei. *J Comp Neurol* 473:377–414.

Reinke H, Wild JM. 1998. Identification and connections of inspiratory premotor neurons in songbirds and budgerigar. *J Comp Neurol* 391:147–163.

Ritchie TLC. 1979. Intratelencephalic visual connections and their relationship to the archistriatum in the pigeon (*Columba livia*). PhD thesis, University of Virginia. Charlottesville, Va.

Schmidt MF, Wild JM. 2014. The respiratory-vocal system of songbirds: Anatomy, physiology, and neural control. *Prog Brain Res* 212:297-335.

Shimizu T, Bowers AN. 1999. Visual circuits of the avian telencephalon: evolutionary implications. *Behav Brain Res* 98:183–191.

Shimizu T, Karten HJ. 2003. The avian visual system and the evolution of neocortex. In: Zeigler HP, Bischoff H-J, editors. *Vision Brain and Behavior in Birds*. Cambridge, MA: MIT Press. pp 103–114.

Shimizu T, Patton TB, Szafranski G, Butler AB. 2008. Evolution of the visual system in reptiles and birds. In Binder MD, Hirokawa N, Windhorst U, Hirsch MC (Eds) *Encyclopedic Reference of Neuroscience*, Heidelberg, Germany: Springer.

Shimizu T, Patton, TB, Husband SA. 2010. Avian visual behavior and the organization of the telencephalon. *Brain Behav Evol* 75:204-217.

Stocker SD, Simmons JR, Stornetta RL, Toney GM, Guyenet PG. 2006. Water deprivation activates a glutamatergic projection from the hypothalamic paraventricular nucleus to the rostral ventrolateral medulla. *J Comp Neurol* 494:

673–685.

Stokes TM, Leonard CM, Nottebohm F. 1974. The telencephalon, diencephalon and mesencephalon of the canary, *Serinus canaria*, in stereotaxic coordinates. *J Comp Neurol* 156:337–374.

Striedter GF. 2005. *Principles of Brain Evolution*. Sunderland, Sinauer.

Striedter GF, Vu ET. 1998. Bilateral feedback projections to the forebrain in the premotor network for singing in zebra finches. *J Neurobiol* 34:27–40.

Vates GE, Broome BM, Mello CV, Nottebohm F. 1996. Auditory pathways of caudal telencephalon and their relation to the song system of adult male zebra finches. *J Comp Neurol* 366:613–642.

Wild JM. 1987a. The avian somatosensory system: connections of regions of body representation in the forebrain of the pigeon. *Brain Res.* 412:205–223.

Wild JM. 1987b. Nuclei of the lateral lemniscus project directly to the thalamic auditory nuclei in the pigeon. *Brain Res* 408:303–307.

Wild JM. 1989. Avian somatosensory system. II. Ascending projections of the dorsal column and external cuneate nuclei in the pigeon. *J Comp Neurol* 287:1–18.

Wild JM. 1990. Peripheral and central terminations of hypoglossal afferents innervating lingual tactile mechanoreceptor complexes in *Fringillidae*. *J Comp Neurol* 298:157–171.

Wild JM. 1994. Visual and somatosensory inputs to the avian song system via nucleus uvaeformis (Uva) and a comparison with the projections of a similar thalamic nucleus in a non-songbird, *Columba livia*. *J Comp Neurol* 349:512–535.

Wild JM. 1997. The avian somatosensory system: The pathway from wing to Wulst in a passerine (*Chloris chloris*). *Brain Res* 759:122–134.

Wild JM. 2004. Functional neuroanatomy of the sensorimotor control of singing. *Ann*

N Y Acad Sci 1016:438-462.

Wild JM. 2008. Birdsong: anatomical foundations and central mechanisms of sensorimotor integration, In: Zeigler HP, Marler, P. (eds) Neuroscience of Birdsong, Cambridge University Press, Cambridge, UK, pp 136–152.

Wild JM, Williams MN. 2000a. Rostral Wulst in passerine birds. I. Origin, course, and terminations of an avian pyramidal tract. J Comp Neurol 416:429-450.

Wild JM, Williams MN. 2000b. A direct cerebrocerebellar projection in adult birds and rats. Neuroscience 96:333-339.

Wild JM, Karten HJ, Frost BJ. 1993. Connections of the auditory forebrain in the pigeon (*Columba livia*). J Comp Neurol 337:32–62.

Wild JM, Kubke MF, Peña JL. 2008. A pathway for predation in the brain of the barn owl (*Tyto alba*): Projections of the gracile nucleus to the “Claw Area” of the rostral Wulst via the dorsal thalamus. J Comp Neurol 509:156–166.

Wild JM, Krützfeldt NOE, Kubke MF. 2010. Connections of the auditory brainstem in a songbird, *Taeniopygia guttata*. III. Projections of the superior olive and lateral lemniscal nuclei. J Comp Neurol 518:2149–2167.

Zeier H, Karten HJ. 1971. The archistriatum of the pigeon: Organization of afferent and efferent connections. Brain Res 31:313-326.

ABBREVIATIONS

AL	Ansa lenticularis
AVT	Ventral area of Tsai
CA	Anterior commissure
Cb	Cerebellum
DM	Dorsomedial nucleus (of ICo)
FA	Fronto-arcopallial tract
GCt	Central grey
GLv	Lateral geniculate nucleus, ventral part
HM	Medial habenular nucleus
DCN	Dorsal column nuclei
DIP	Dorsointermediate nucleus of the posterior thalamus
DIVA	Nucleus intermedius ventralis anterior
DM	Dorsomedial nucleus of the Intercollicular complex
DSO	Supraoptic decussation
E	Entopallium
FA	Fronto-arcopallial tract
FPL	Lateral forebrain bundle
GCt	Central grey
GLv	Ventral part of lateral geniculate nucleus
GP	Globus pallidus
HA	Apical hyperpallium
HM	Medial habenular nucleus
IA '0'	Inter-aural zero
ICo	Intercollicular nucleus

Imc	Magnocellular part of the isthmic nucleus
Ipc	Parvocellular part of the isthmic nucleus
L2	Thalamorecipient part of Field L
LaM	Mesopallial lamina
LM	Nucleus lentiformis mesencephali
LPS	Pallio-subpallial lamina
LSt	Lateral striatum
M	Mesopallium
MLd	Lateral mesencephalic nucleus, dorsal part
MSt	Medial striatum
N	Nidopallium
nBOR	Nucleus of the basal optic root
NI	Intermediate nidopallium
Nif	Nucleus interface
NIII	Third cranial nerve
OM	Occipitomesencephalic tract
Ov	Nucleus ovoidalis
PAm	Nucleus parambigualis
PL	Lateral pontine nucleus
PM	Medial pontine nucleus
PT	Pretectal nucleus
PV	Posteroventral thalamic nucleus
PVM	Periventricular magnocellular nucleus
QT	Quintofrontal tract
rf	Reticular formation

RSd	Superior reticular nucleus of the thalamus, dorsal part
RSv	Superior reticular nucleus of the thalamus, ventral part
Rt	Nucleus rotundus
Ru	Red nucleus
rUva	Rostral part of nucleus uvaeformis
Sp	Nucleus subpretectalis
SLu	Nucleus semilunaris
SpA	Subpallial nucleus of the arcopallium
SpL	Nucleus spiriformis lateralis
SpM	Nucleus spiriformis medialis
SRt	Nucleus subrotundus
TeO	Optic tectum
TFM	Fronto-thalamic and thalamo-frontal tract
TOv	Tractus ovoidalis
TrO	Optic tract
TSM	Septomesencephalic tract
TT	Tecto-thalamic tract
Uva	Nucleus uvaeformis
V	Ventricle
vf	Ventral funiculus
VeS	Superior vestibular nucleus

FIGURE LEGENDS

Figure 1. Neural responses evoked by a light flash to the contralateral eye.

A-F: Schematic coronal hemisections showing the location of recordings – indicated by asterisks - made from PL (A), rUva (B), and throughout the intermediate nidopallium (C-F). The rostrocaudal levels of the recordings are shown in the sagittal schematic of the zebra finch brain at top left. a-f: Scope records of evoked neural activity. a: an average of 50 responses from **a** in A to stimulus presentation at 1 per second; b: a single response from **b** in B; c1: a single response (filters completely open) from **c1** in C; c2: a single response from **c2** in C. d1, d2: single responses from **d1** and **d2** in D; e1: an average of 50 responses from **e1** in E; e2: a single response from **e2** in E; f: a single response from **f** in F. Scale bars at bottom left = 1 mm.

Figure 2.

Ascending anterograde labeling resulting from an iontophoretic injection of BDA in PL. A: Schematic drawing of a transverse section showing the center of the injection (solid black in the box a1, with spread from the injection shaded.) a1: photomicrograph of the BDA injection in PL – center depicted by an asterisk. a2: area corresponding to the a2 box in A. Fiber and terminal labeling in the lateral and dorsal part of Uva, leaving the core of the nucleus unlabeled. B: The boxed area is shown as a corresponding photomicrograph in b, with the fiber and terminal labeling in the rostral pole of Uva, dorsal to SpM (Nissl counterstained section). C: The boxed area is shown as a corresponding photomicrograph in c, with the fiber and terminal labeling in rUva surrounding the lateral aspect of Ov. D: The large boxed area is shown as a corresponding photomicrograph in d, with the anterograde label forming an ascending strip lateral to TOv and Ov. The strip also contains some retrogradely

labeled cells; see also figure 4G. E: The boxed area is shown as a corresponding photomicrograph in e, which shows diffuse, fine fiber and terminal labeling throughout SpA. Calibration bars = 200 μm for a1, b, c, and e; ; 100 μm for a2; 500 μm for d.

Figure 3.

A: Camera lucida drawing of the distribution of retrogradely labeled neurons (one dot = one neuron) primarily in the tectum resulting from an injection of CTB in rUva, shown as solid black lateral to Ov, with spread from the injection indicated by surrounding shading. B: Photomicrograph of a Nissl stained section having the same area, approximate rostrocaudal level and location as the box in A. C: Photomicrograph of retrogradely labeled neurons in the tectum resulting from the injection depicted in A. D: Ditto for the contralateral tectum, but in which labeled neurons are confined to layer 13. Also visible is anterograde labeling in rUva resulting from somatopetal and somatofugal transport of CTB, to and from retrogradely labeled ipsilateral tectal neurons. E: Retrograde and anterograde labeling in PL resulting from the injection shown in A. Note that the retrogradely labeled neurons mostly lie external (ventral) to the anterograde labeling, the source of which is probably tectal and not rUva neurons (see text). F: Retrograde and anterograde labeling in PL resulting from a BDA injection in rUva (counterstained section) – again note the more ventral location of most of the retrogradely labeled neurons. Calibration bars: 200 μm for B, 500 μm for C and D, 100 μm for E and F.

Figure 4

A-F: Retrograde labeling of different types of neurons in different regions and

rostrocaudal levels of the right tectum resulting from the BDA injection depicted in figure 2 (see text). A: section showing labeling throughout almost the complete tectum at a level rostral to the anterior commissure; B: the dorsolateral tectum; C: the ventrolateral tectum; D and F: the ventromedial tectum; E: the ventral tectum. B, C, D and E are lightly counterstained; A and F are uncounterstained. The arrow in C points at a labeled neuron in layer 6. Note the layers 8 and 9 neurons, e.g., in C, D and F, that extend their processes out to layer 4, where they terminate as small lateral arbors - see also a1 in figure 2. G: Anterograde and retrograde labeling in the strip lateral to TOv and at the base of the strip, dorsolateral to nBOR. H: Retrogradely labeled neurons in the center of the intermediate arcopallium. Calibration bars = 200 μm for A, B, F, G and H; 100 μm for C-E.

Figure 5.

A: Anterograde and retrograde labeling resulting from a CTB injection made through the stratum opticum of the right tectum and covering the outer dozen laminae. B: Fiber and terminal labeling in the lateral and dorsal parts of Uva, leaving the caudal core unlabeled. C: A more rostral section than shown in A, showing fiber and terminal labeling in rUva. D: Fiber and terminal labeling in the inner (dorsal) part of PL. Calibration bars = 500 μm for A and C; 200 μm for B and 100 μm for D.

Figure 6.

A-D: Anterograde labeling caudal to an injection of BDA in PL. A: in the ventrolateral pons; B: in the ventral funiculus of an upper cervical spinal segment; C: fibers in the spinal lemniscus entering the lateral cerebellum; D: terminations of mossy fiber parasagittal bands in the cerebellum. E: Retrogradely labeled neurons in PL

resulting from an injection of CTB in the caudal cerebellar folia. F: Retrogradely labeled neurons in PL resulting from injections of Fast Blue in the caudal cerebellum (blue neurons) and CTB Alexa 555 in rUva (orange-red neurons). Note also the substantial anterograde labeling resulting from the rUva injection (but see text).

Figure 7.

Camera lucida drawings of four pairs of right transverse hemisections (A,B; C,D; E,F; G,H) depicting the location of BDA injections involving Uva and rUva (solid black in A, C, E, G) and corresponding terminal fields resulting from those injections in B, D, F, and H.

Figure 8.

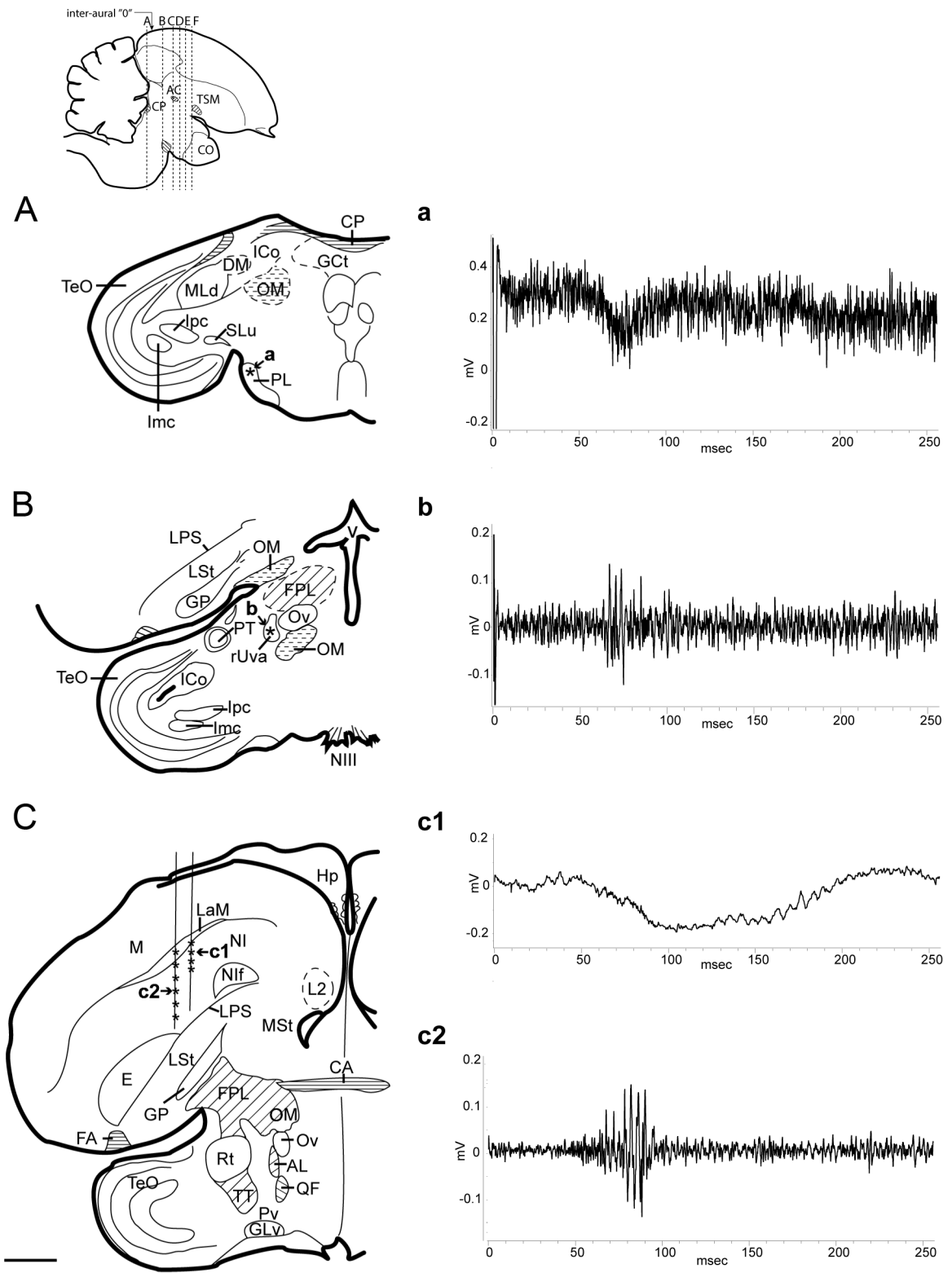
A,B: an injection of 10k BDA in rUva (A) and the resulting terminal field in the nidopallium (B). C,D: an injection of 3k BDA in the nidopallium bordering the dorsomedial entopallium (C), and the resulting retrogradely labeled neurons in rUva (D). E,F: a CTB injection in the nidopallium bordering the dorsomedial entopallium (E), and the resulting retrogradely labeled neurons in rUva (F, section counterstained with Neutral Red). G: anterograde labeling in the ventral mesopallium resulting from the BDA injection shown in C. H: anterograde labeling in the lateral striatum resulting from a CTB injection adjacent to the LPS. Similar anterograde labeling can also be seen in E. Calibration bars = 200 μm for A, B, F, G, and H; 100 μm for D; 500 μm for C and E.

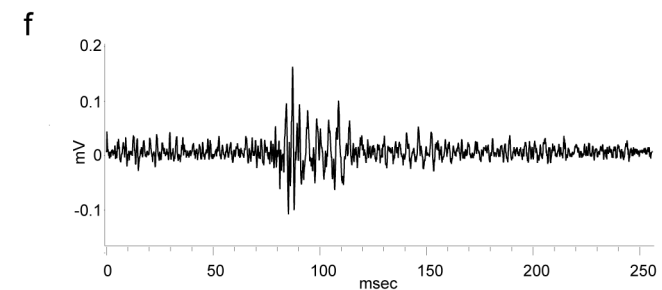
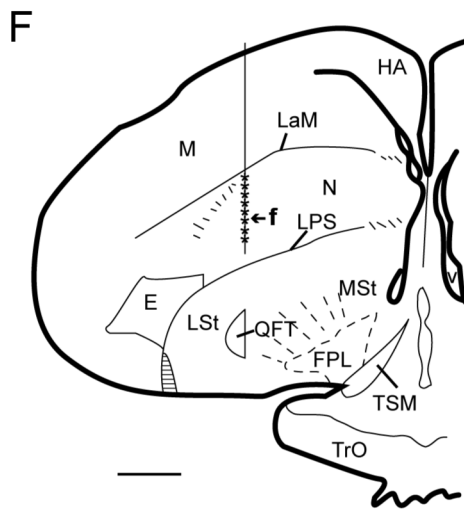
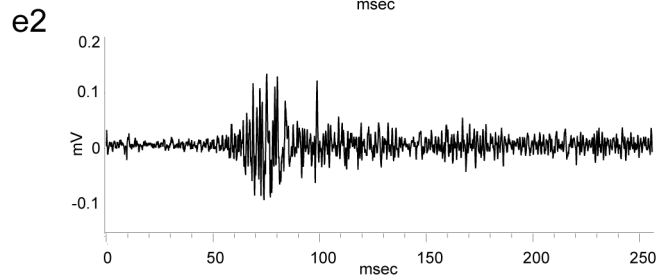
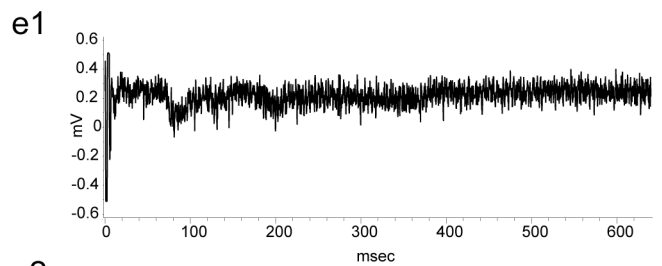
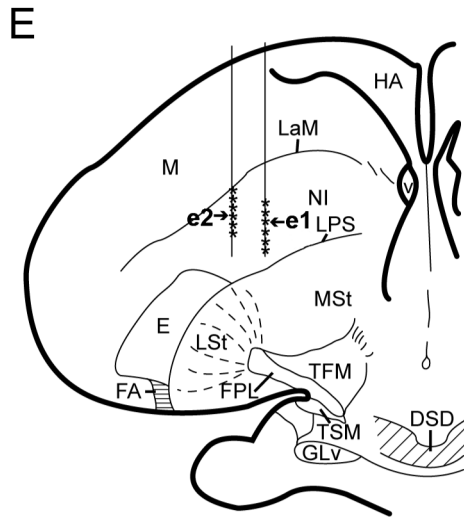
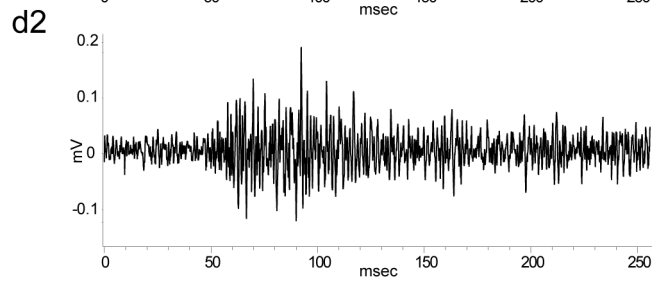
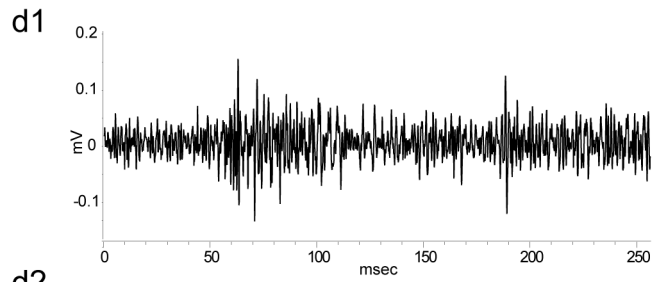
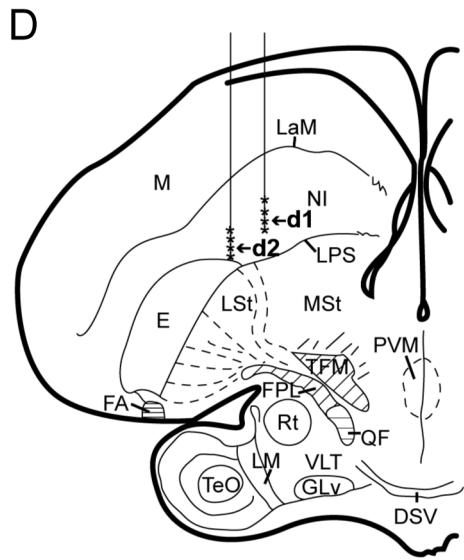
Figure 9.

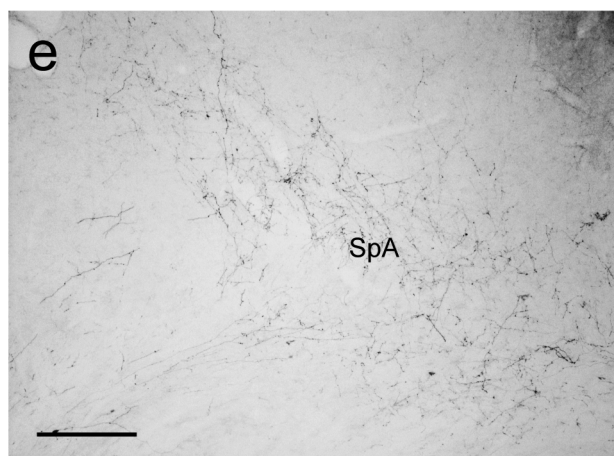
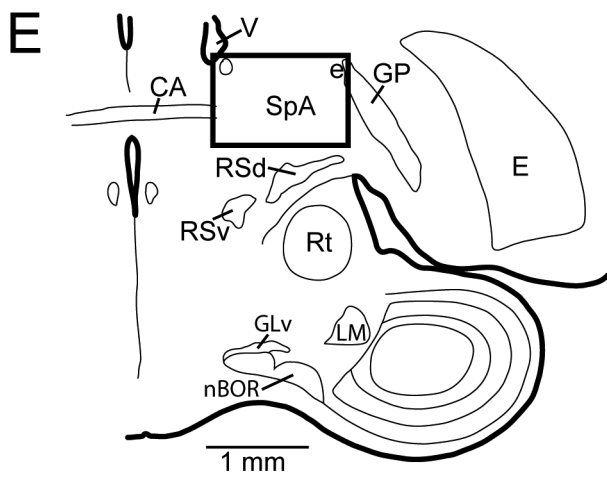
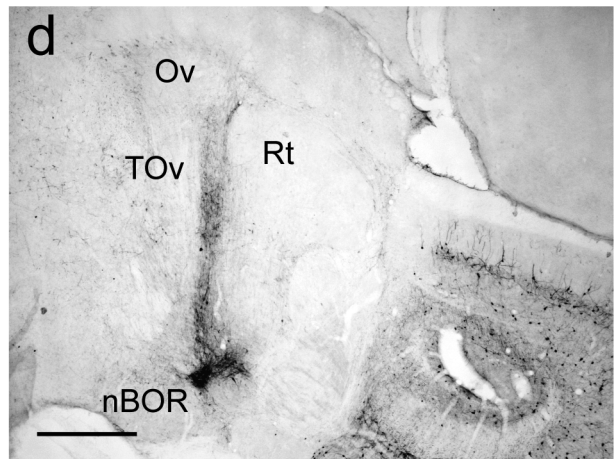
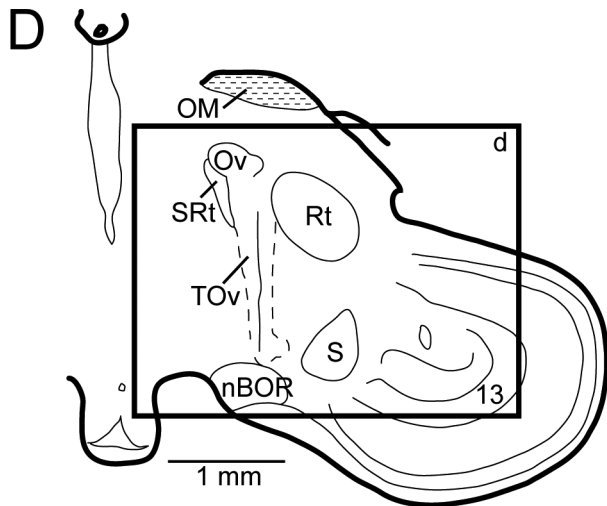
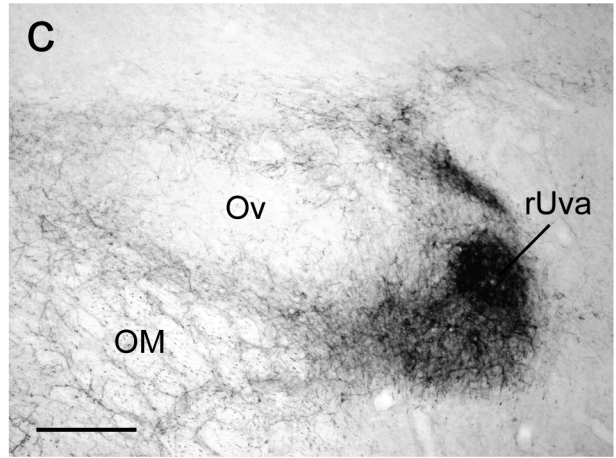
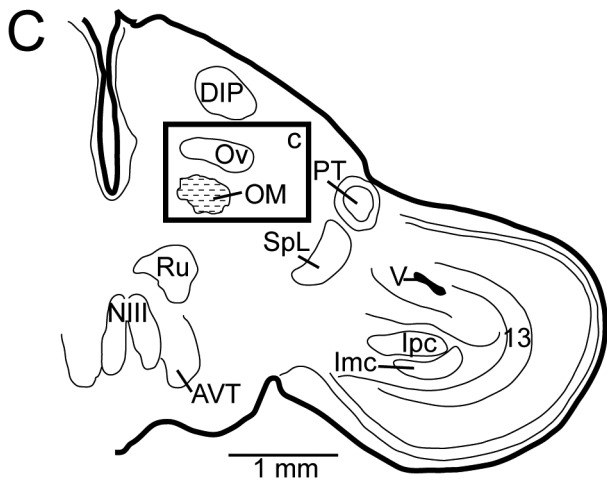
A: Schematic depiction of the Uva/rUva complex from caudal Uva through rUva, a

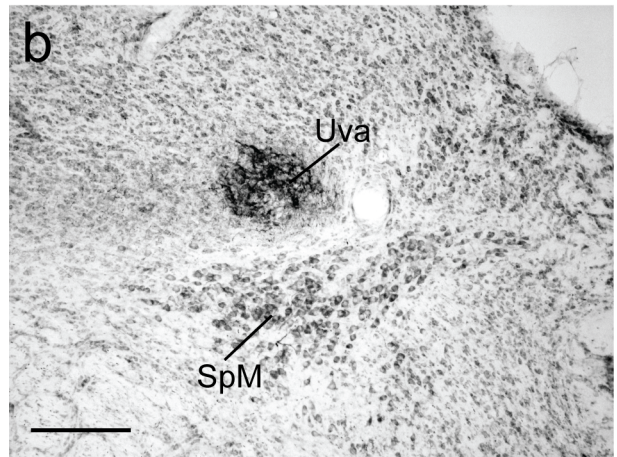
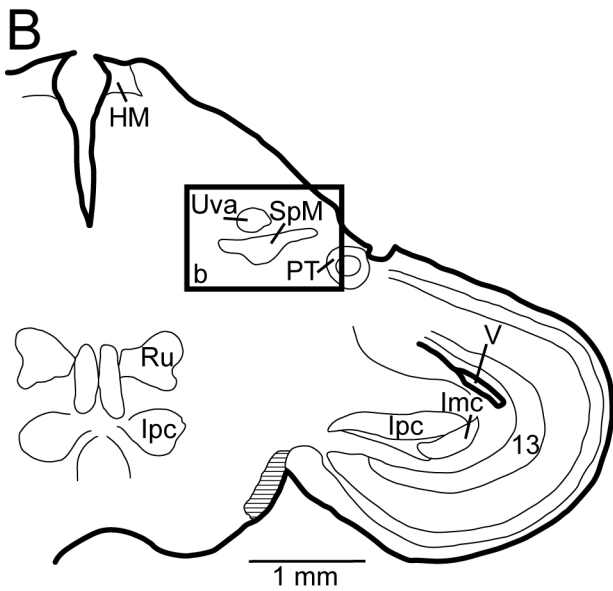
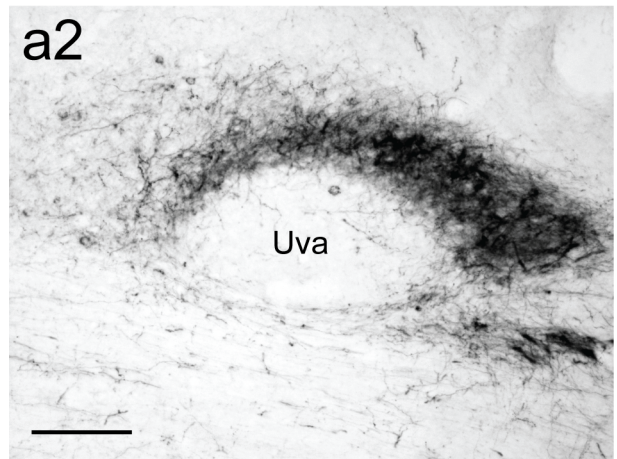
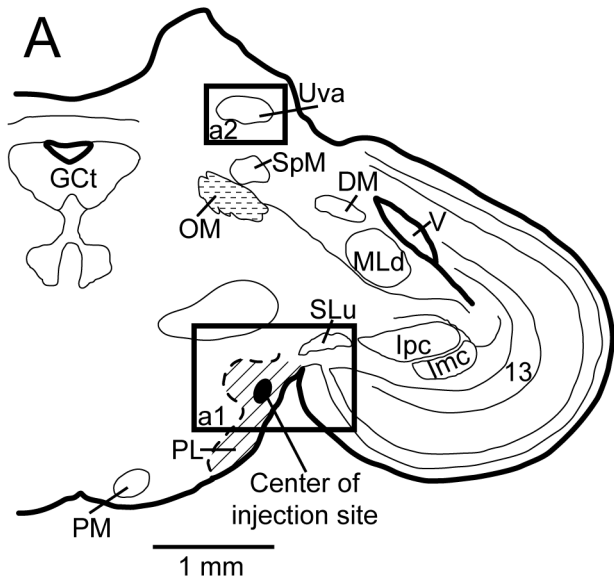
distance of ~0.5 mm. The various sensory inputs to parts of the complex are indicated.

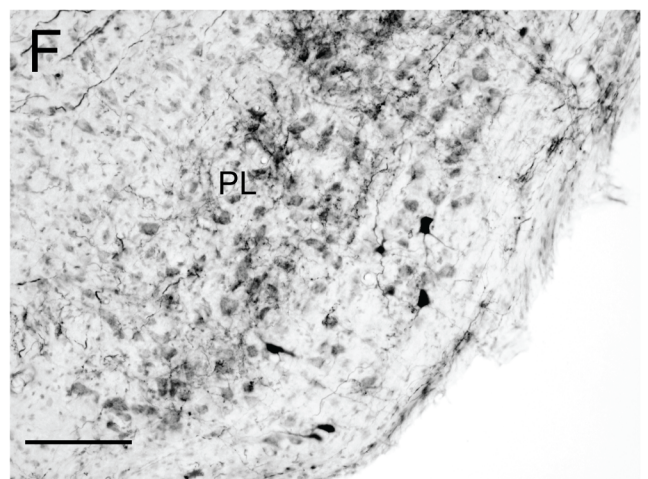
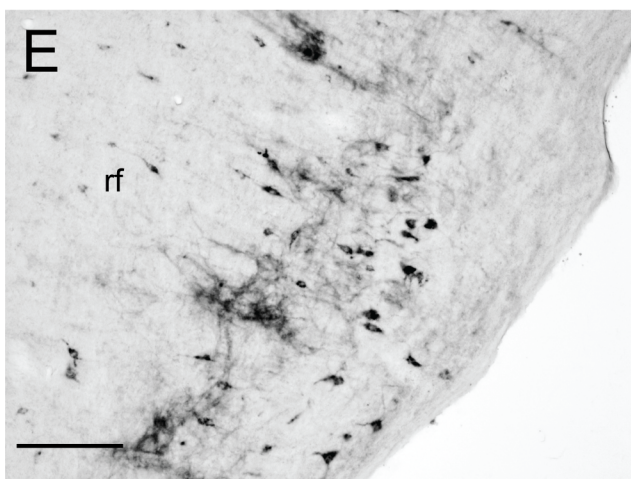
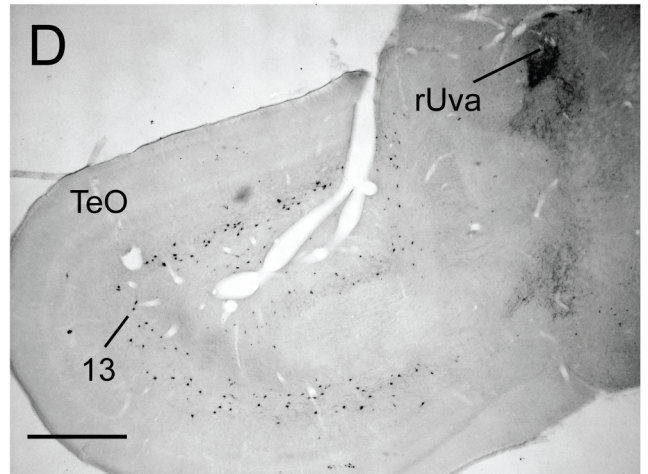
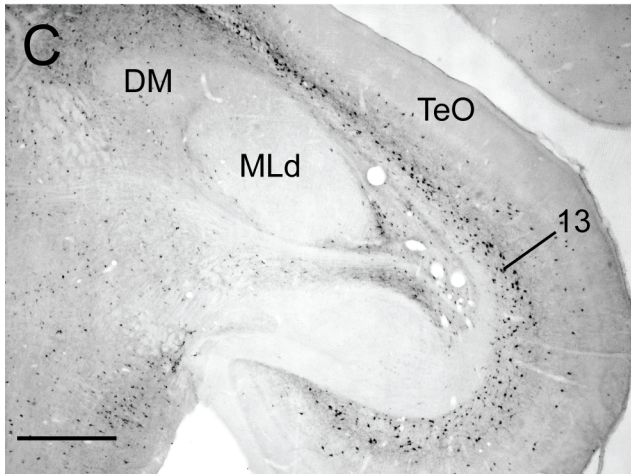
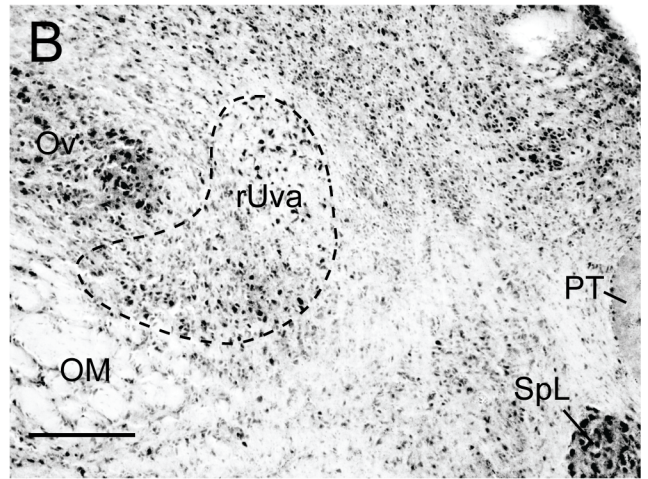
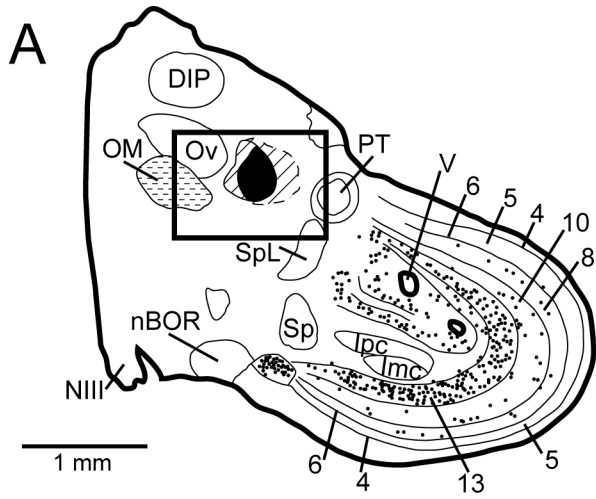
B: Schematic depiction of the two tectofugal pathways, the first being depicted with solid arrows, and the second, reinforced by lateral pontine projections, with dashed arrows.

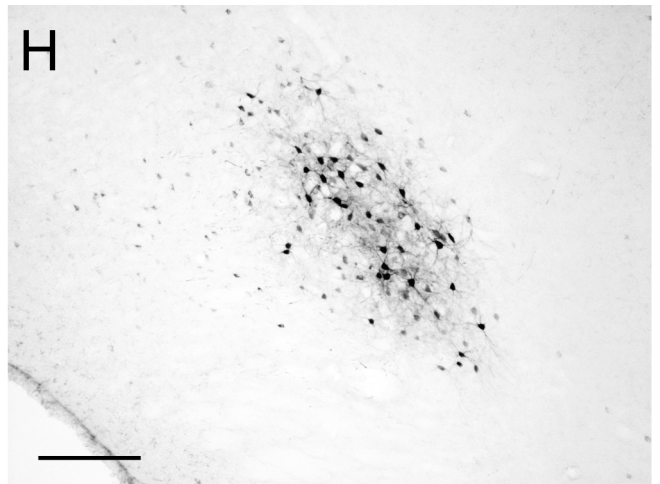
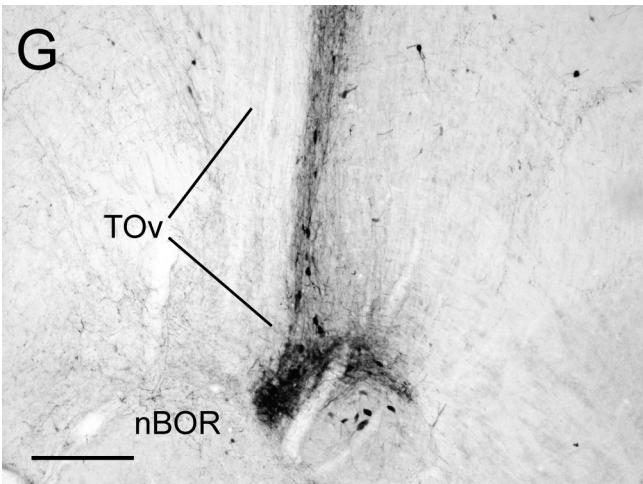
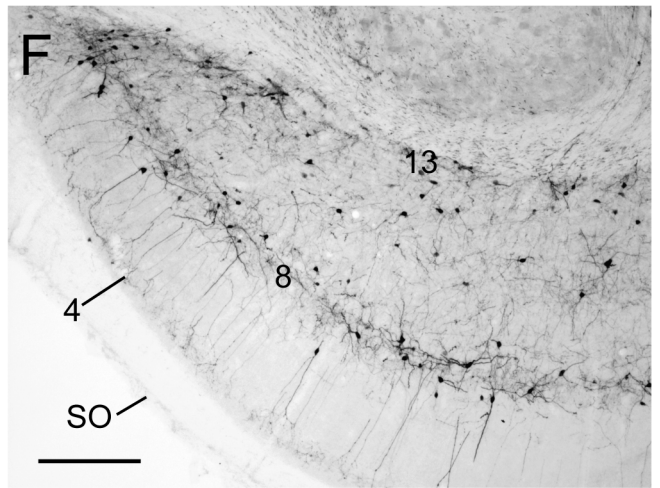
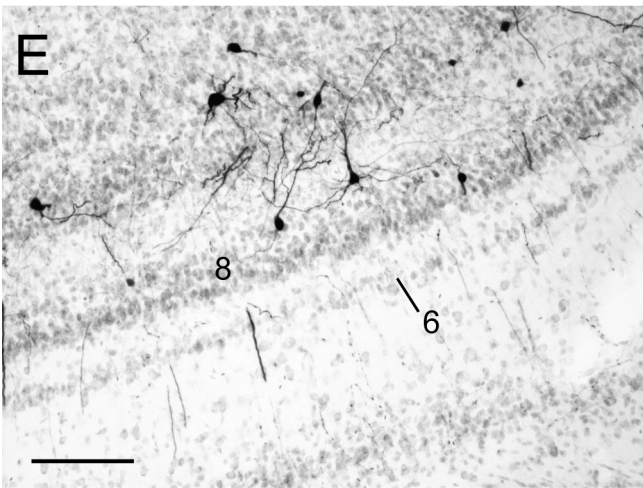
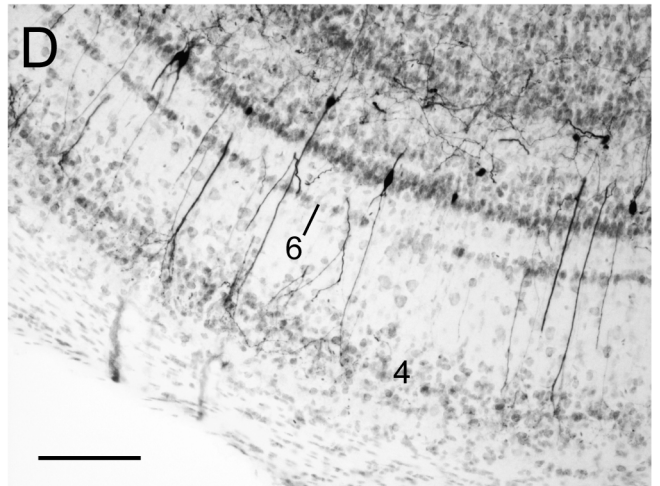
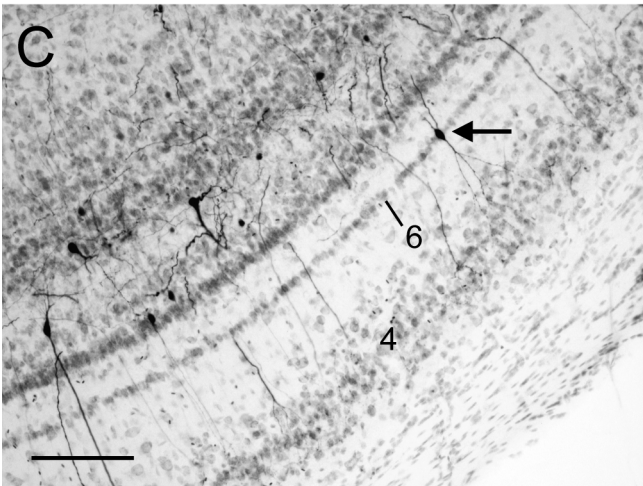
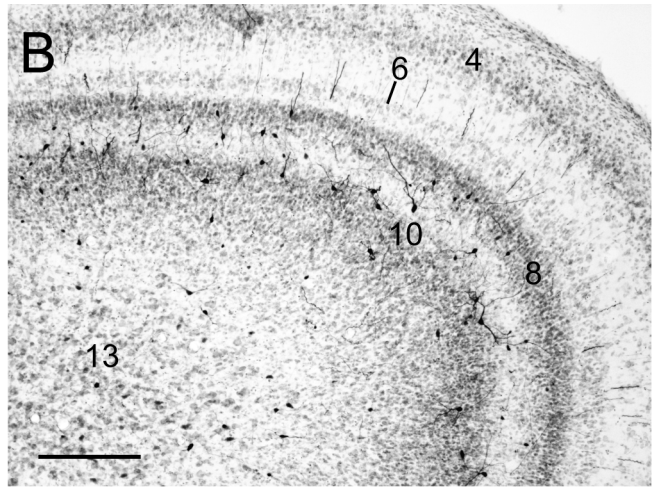
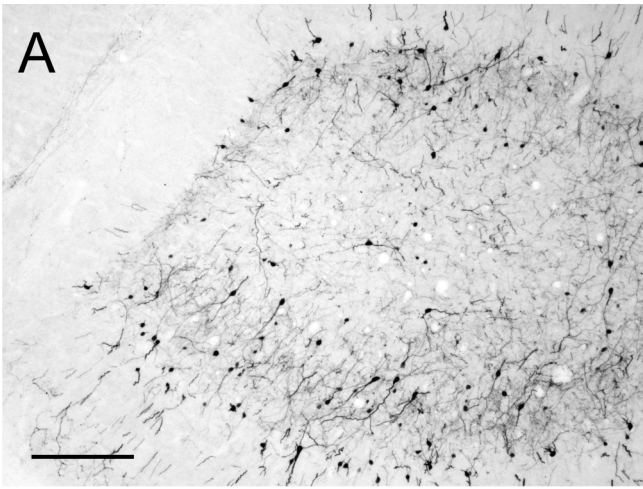


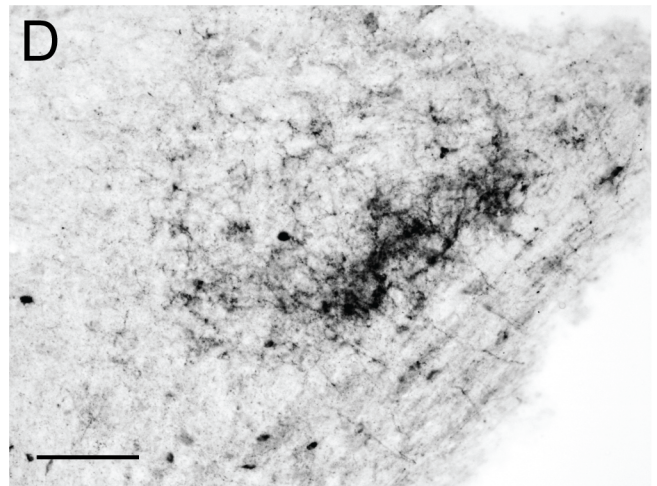
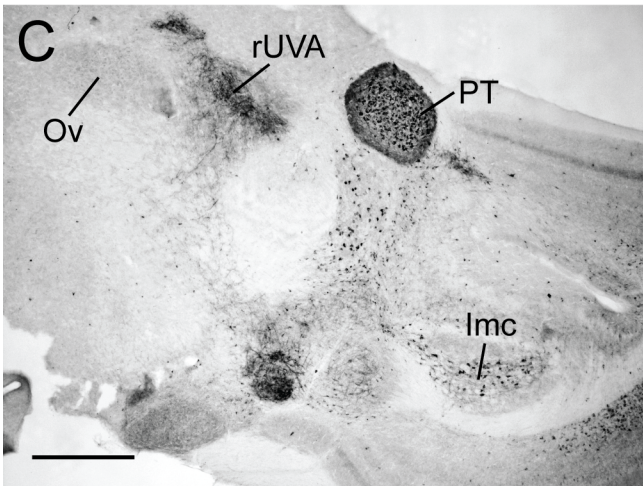
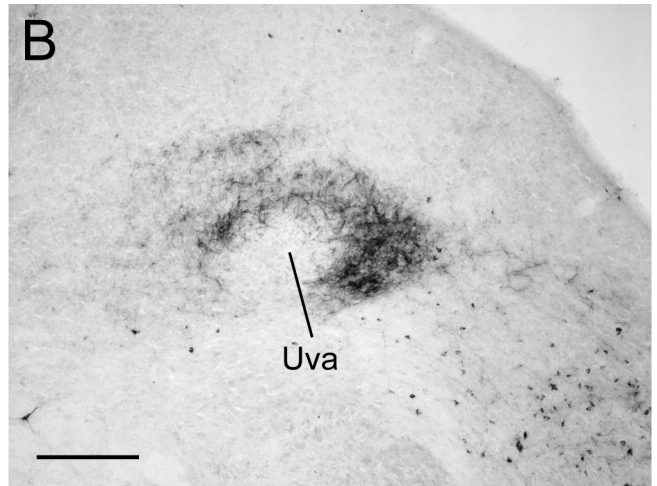


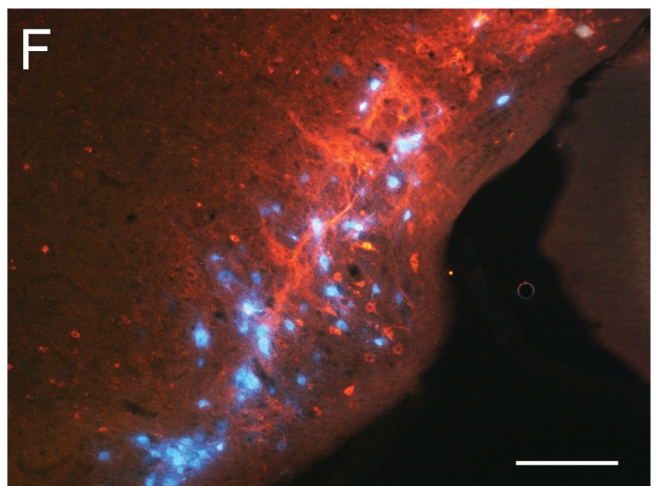
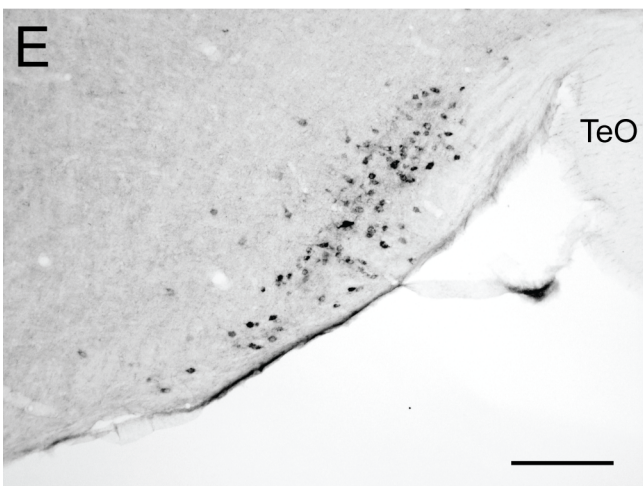
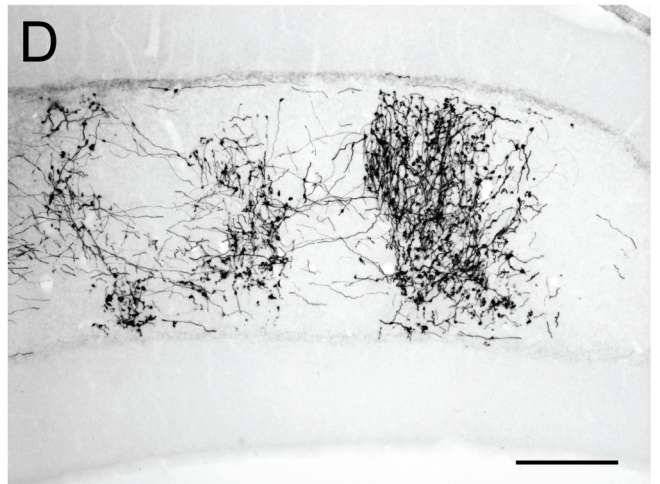
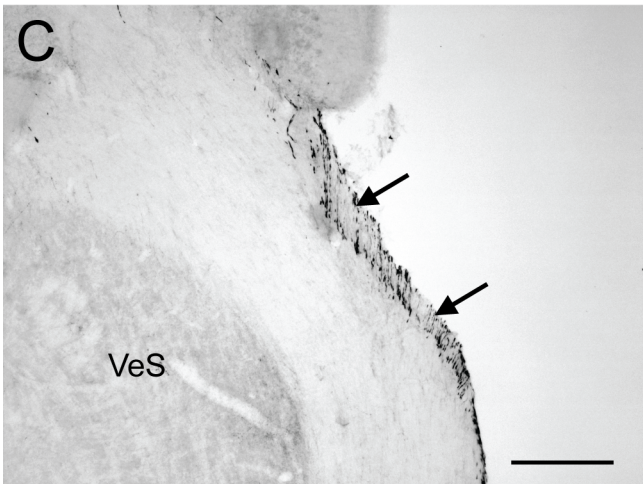
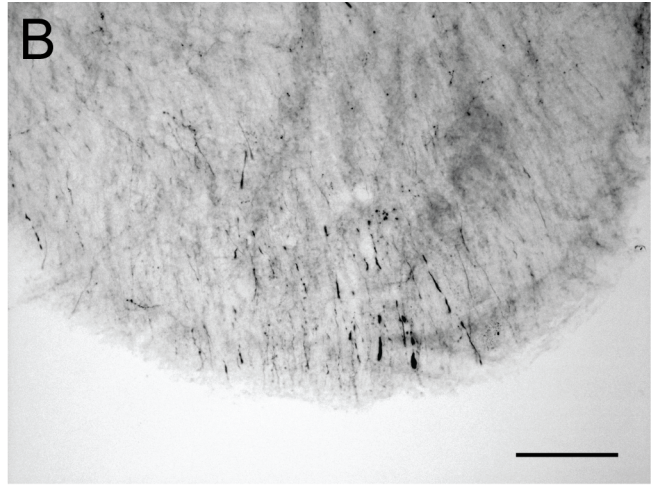
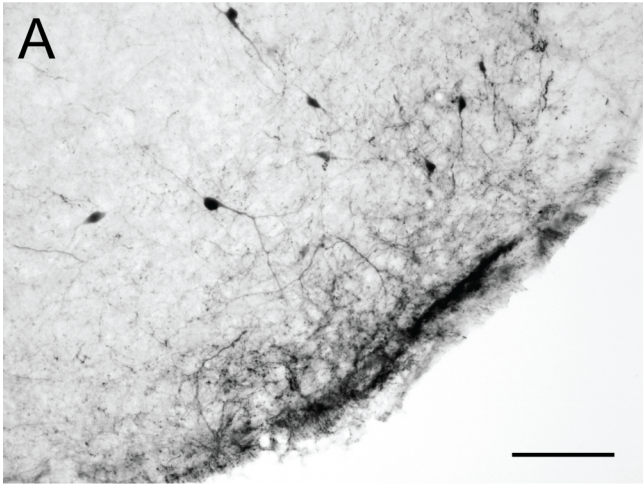


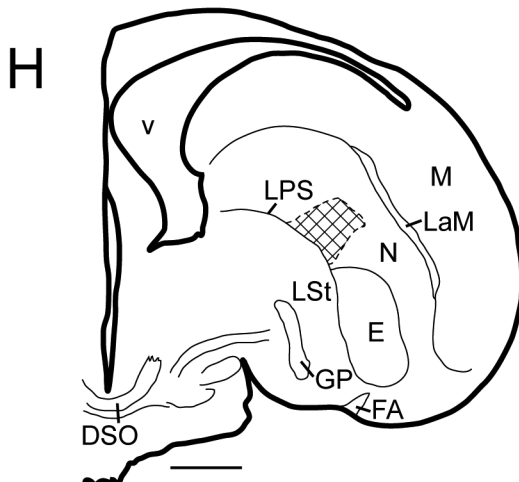
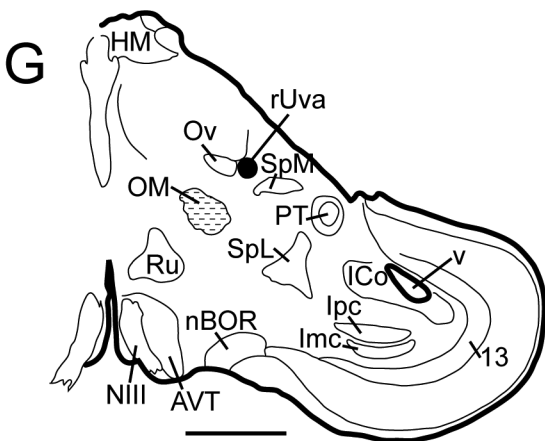
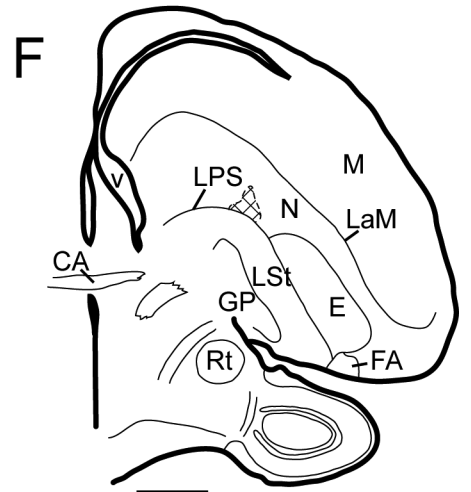
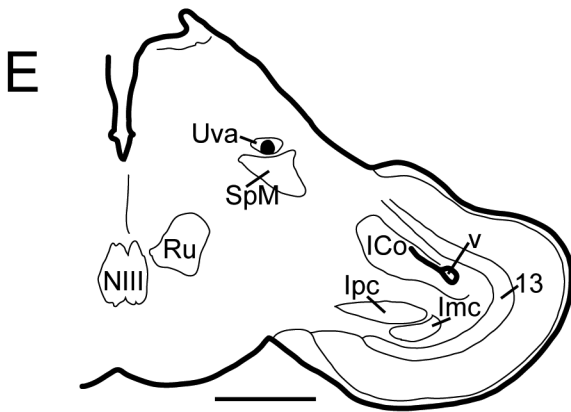
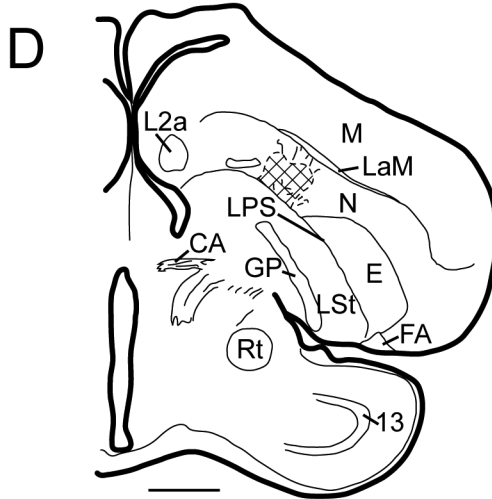
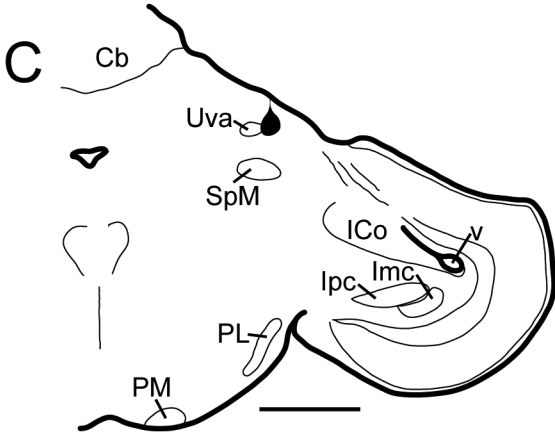
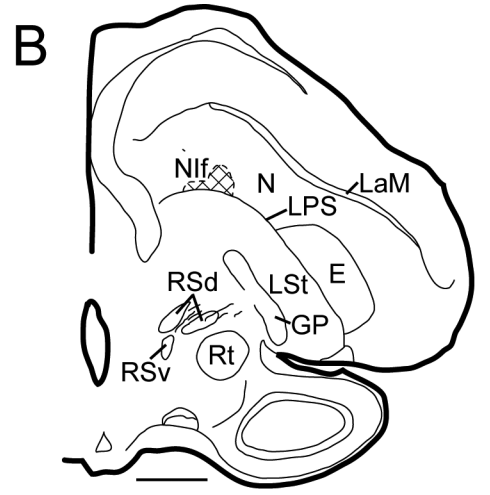
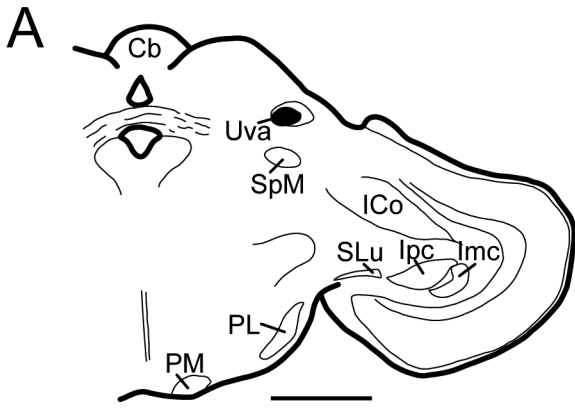


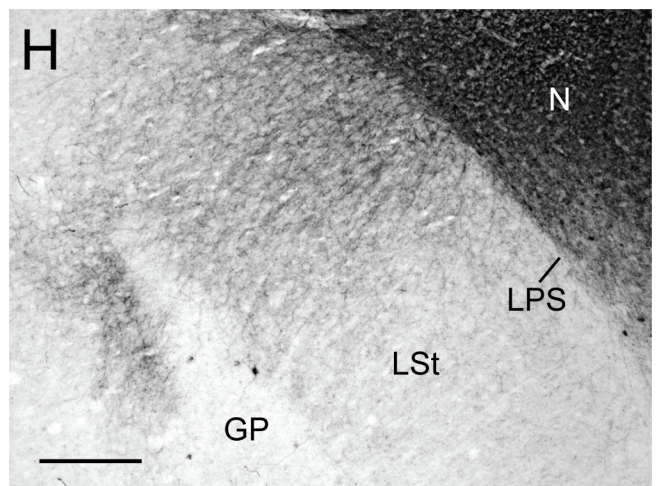
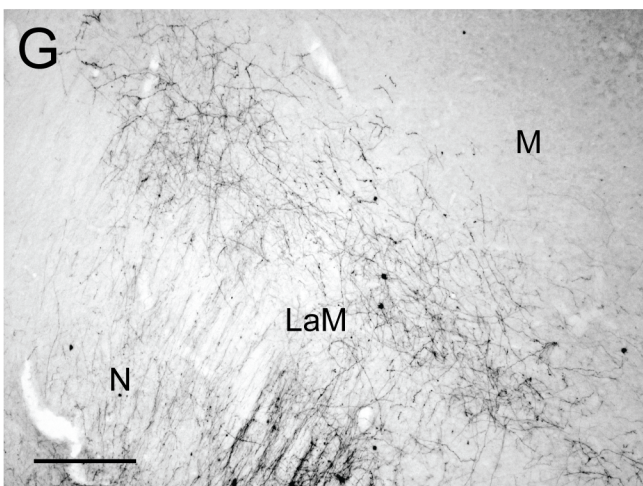
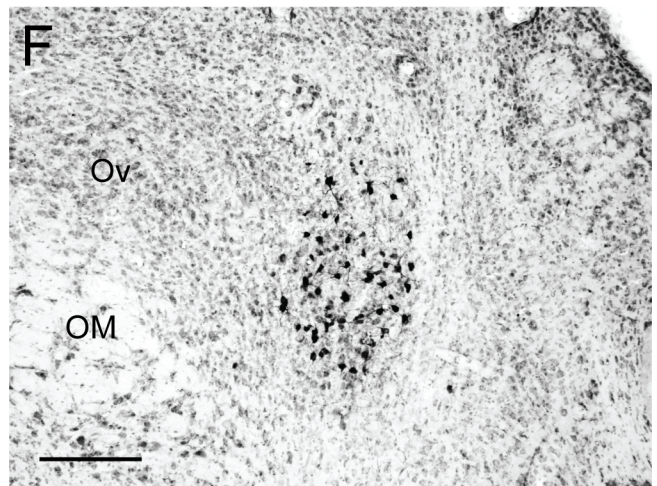
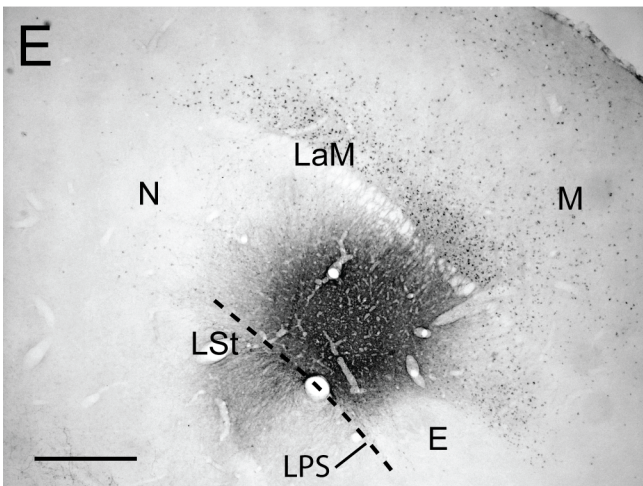
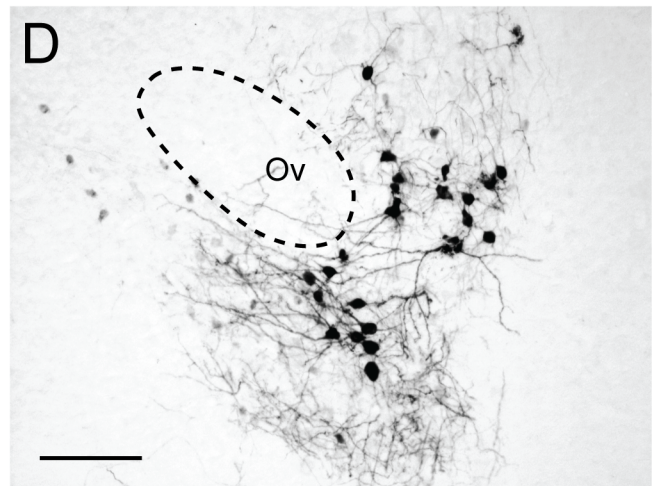
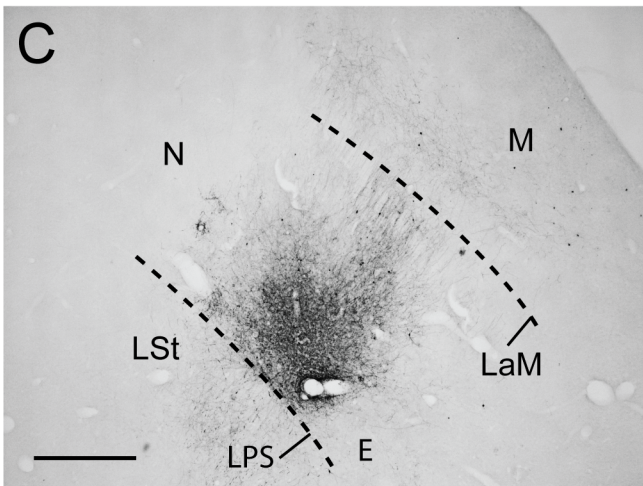
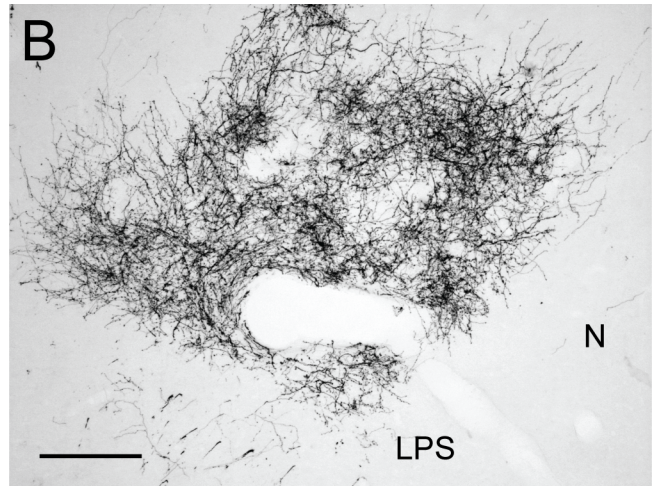
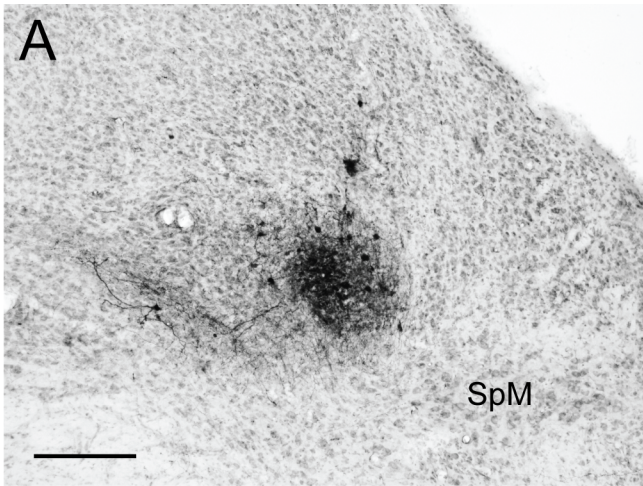




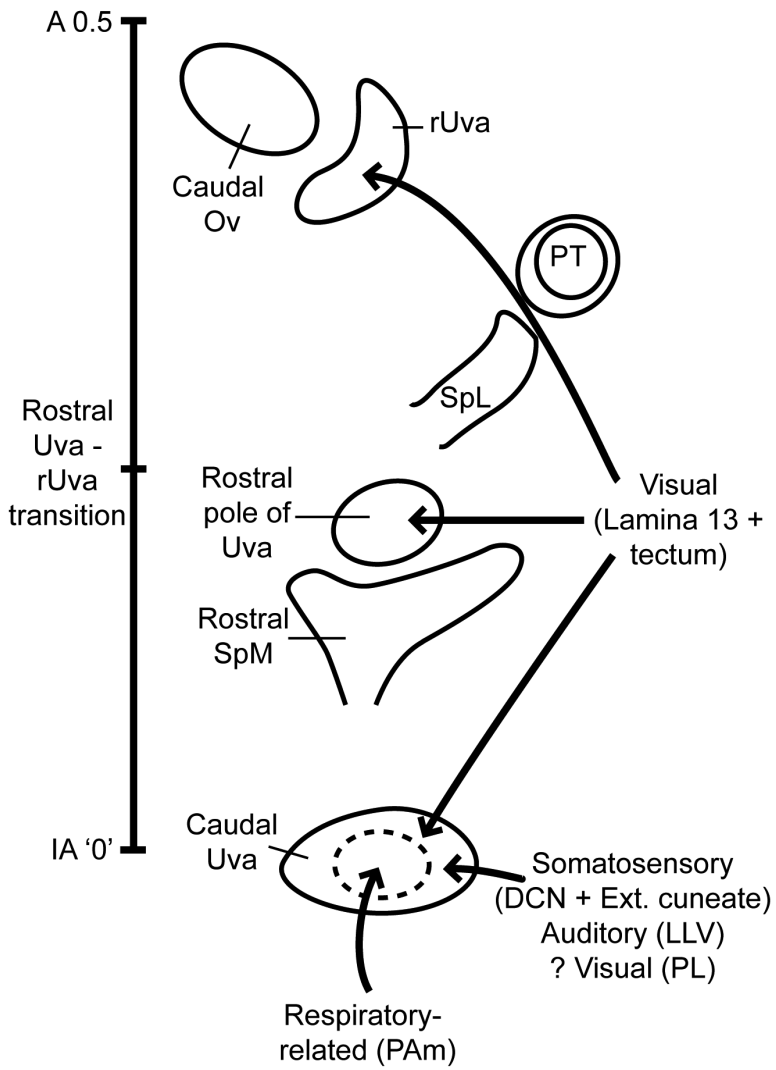








A



B

